Accepted Manuscript

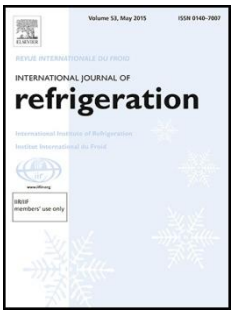

Title: Two-phase frictional pressure drop in horizontal micro-scale channels: experimental data analysis and prediction method development

Author: Daniel Felipe Sempértegui-Tapia, Gherhardt Ribatski

PII: S0140-7007(17)30132-9
DOI: http://dx.doi.org/doi: 10.1016/j.ijrefrig.2017.03.024
Reference: JIJR 3599

To appear in: *International Journal of Refrigeration*

Received date: 23-2-2017
Revised date: 20-3-2017
Accepted date: 25-3-2017

Please cite this article as: Daniel Felipe Sempértegui-Tapia, Gherhardt Ribatski, Two-phase frictional pressure drop in horizontal micro-scale channels: experimental data analysis and prediction method development, *International Journal of Refrigeration* (2017), http://dx.doi.org/doi: 10.1016/j.ijrefrig.2017.03.024.

TWO-PHASE FRICTIONAL PRESSURE DROP IN HORIZONTAL MICRO-SCALE CHANNELS: EXPERIMENTAL DATA ANALYSIS AND PREDICTION METHOD DEVELOPMENT

Daniel Felipe Sempértegui-Tapia[a*] and Gherhardt Ribatski[b]

[a] College of Engineering, Design and Physical Science, Brunel University of London, Uxbridge, London, UK.

[b] Heat Transfer Research Group, Escola de Engenharia de São Carlos (EESC), University of São Paulo (USP), São Carlos, SP, Brazil.

* Corresponding author.

E-mail adresses: Brunel University of London, Uxbridge, London, UB8 3PH, UK

dsempertegui@hotmail.com (D.F. Sempértegui-Tapia)

Tel: +44 1895268560,

HIGHLIGHTS

- Experimental data for adiabatic frictional pressure drop in a single microchannel.
- Characteristic dimension discussion to evaluate pressure drop inside microchannels.
- Parametric analysis and comparison of the data with predictive methods.
- Proposition of a new predictive method for two-phase pressure drop.
- Proposed method provides accurate predictions of present and independent databases.

ABSTRACT

An investigation was conducted on the effects of fluid refrigerant and channel geometry on the frictional pressure drop during two-phase flow inside microchannels. Experimental results for two-phase frictional pressure drop were obtained for the refrigerants R134a, R1234ze(E), R1234yf and R600a in a circular channel and for R134a in square and triangular channels. The experiments were performed for mass velocities from 100 to 1600 kg m^{-2} s^{-1}, saturation temperatures of 31 and 41°C, and vapor qualities from 0.05 to 0.95. The experimental data have been analyzed focusing on the effects of the geometry and fluid on the two-phase pressure drop. Then, the data were compared with the most quoted predictive methods from literature. Based on the broad database obtained, a new method for prediction of the two-phase frictional pressure drop was proposed. The new method provided accurate predictions of the database, predicting 89% of the results within an error band ±20%.

Keywords: two-phase flow, geometry effect, pressure drop, convective boiling, microchannels

NOMENCLATURE

A	Area, m².
C_C	Area ratio vena contracta, dimensionless.
dp/dz	Pressure drop gradient, kPa m^{-1}
D	Diameter, m.
f	Friction factor, dimensionless.
G	Mass velocity, kg m^{-2} s^{-1}.
i	Enthalpy, J kg^{-1}.
K	Singular pressure drop coefficient, dimensionless.
k	Momentum correction factor, dimensionless.
L	Length, m.
M	Mass flow rate, kg s^{-1}.
p	Pressure, kPa.
P	Electrical power, W.
Ra	Arithmetic mean roughness, µm.
Re	Reynolds number, dimensionless.
Rt	Maximum roughness height, µm.
x	Vapor quality, dimensionless.
z	Position along the tube, m.

Greek letters

α	Void fraction, dimensionless.
β	Energy momentum coefficient, dimensionless
η	Parcel of data predicted within a certain error band, %.
λ	Empirical coefficient, dimensionless.
μ	Dynamic viscosity, Pa.s.
ρ	Density, kg/m³.
ς	Aspect ratio for rectangular channels, dimensionless.
σ_A	Area ratio of contraction/expansion, dimensionless.
ω	Empirical coefficient, dimensionless.

Subscripts

1ϕ	Single-phase
2ϕ	Two-phase
Ac	Accelerational.
con	Contraction
exp	Expansion
Eq	Equivalent
f	Frictional
in	Inlet
int	Internal
I	Irreversible
H	Hydraulic
L	Liquid
L0	Two-phase mixture as liquid
G	Vapor
LG	Difference between vapor and liquid properties
G0	Two-phase mixture as vapor
out	Outlet
ph	Pre-heater
pred	Predicted
R	Reversible
sat	Saturation
ts	Test section.
vs	Visualization section

1. *INTRODUCTION*

In the last years, several experimental studies concerning two-phase pressure drop were performed and, as consequence, new predictive methods were proposed with most of them based on restricted experimental databases. However, as pointed out by Ribatski (2013), there are still differences among data from independent laboratories that can be related to several aspects, e.g. different surface roughness, channel dimension uncertainties, channels obstructions, inappropriate data reduction procedures and the presence of thermal instabilities (see also Ribatski et al. (2007)).

According to the comprehensive literature review by Tibiriçá and Ribatski (2013), almost 97% of the studies concerning single-channels were performed for circular cross sections, especially, due to the easiness to obtain them in the market in different diameters. However, the two-phase flow behavior in a circular microchannel may be significantly different than for non-circular cross-sectional geometries (square, rectangular, triangular, etc.) due to factors like aspect ratio and a possible accumulation of liquid in the corners with the subsequent decreasing of the liquid film thickness in the region between consecutive vertices. It is also important to emphasize that the characteristic dimension of the channel that should be adopted to predict frictional pressure drop during two-phase flows in non-circular channels is still not clear in the literature.

Microchannel array heat sinks evaluated in the literature are generally formed by rectangular microchannels. This fact is evidenced by the study of Tibiriçá and Ribatski (2013). According to these authors, 87% of studies concerning multi-channels configurations were performed for rectangular cross sections covering a wide range of aspect ratios and only 9% for triangular cross sections. It is important to mention that experimental data for pressure drop in microchannel arrays may be affected by

instabilities, local restrictions, maldistribution and back flow, just to name a few effects. Therefore, all these phenomena that are typical of the array geometry make difficult to isolate the frictional pressure drop caused by the two-phase flow along the channel. For this reason, the present authors believe that pressure drop experimental data obtained for microchannel arrays are not suitable to be used in the development of predictive method with generic claims.

It should be mentioned that the majority of studies concerning the evaluation of the two-phase pressure drop in small diameter channels was performed for HFC refrigerants (see Kim and Mudawar (2014)). In 1997, the Kyoto Protocol has established the gradual replacement of HFCs by refrigerants with global warming potential (GWP) less than 150. In this context, a new demand was generated for fluids that could substitute the HFCs. According to Calm (2008) and Mota-Babiloni et al. (2014), the potential substitutes for HFCs are natural refrigerants (hydrocarbons, CO_2 and ammonia), hydrofluoroolefins (HFOs) and mixtures of HFCs and HFOs.

In the last few years, some studies concerning natural refrigerants and HFOs were reported in the literature. However, the majority of these studies were performed for macro-scale channels (D>3mm). Moreover, it is still not clear if the predictive methods available in the literature are capable to predict pressure drop and the HTC of these fluids. Table 1 describes studies from literature concerning the evaluation of two-phase pressure drop of low GWP refrigerants in micro-scale channels. Pamitran et al. (2010), Wu et al. (2011) and Huang et al. (2016) obtained results for pressure drop under flow boiling conditions. Among 11 methods evaluated by them, Pamitran et al. (2010) found that the homogeneous model with the two-phase viscosity given by Beattie and Whalley (1982) provides the best predictions of their data. Instead, Huang et al. (2016) pointed out the predictive method of Kim and Mudawar (2012) as the most

accurate one. Pamitran et al. (2010), Huang et al. (2016), Ducoulombier et al. (2011) and Del Col et al. (2013) proposed new predictive methods based on their experimental data. The predictive method developed by Del Col et al. (2013) predicted reasonably well the data presented by Del Col et al. (2013, 2014, 2015). It is important to notice in Table 1 that only one study was performed for the refrigerants R1234yf and R1234ze(E) in single microchannels. It should be also highlighted that according to the best of the author's knowledge, experimental studies on pressure drop in micro-scale channels for isobutane are not available in the open literature.

The aspects above mentioned indicate the need of performing careful experiments and obtaining accurate data for a wide range of cross-sectional geometries and fluids in order to support the development of accurate predictive methods. In this context, the present paper concerns an experimental investigation on the effect of channel geometry and working fluid on the two-phase frictional pressure drop gradient under adiabatic conditions. The experiments were performed for horizontal single-channels. Two-phase frictional pressure drop data were obtained for the fluids R134a, R1234ze(E), R1234yf and R600a in a circular channel. Data for R134a were also obtained for square and triangular channels. Focusing on maximizing the number of channels and, consequently the effective heat transfer area, keeping the volume of a 3-D heat sink, the evaluated channels presents the same external perimeter and, therefore, different equivalent diameters of 1.1, 0.977 and 0.835 mm for circular, square and triangular cross-sectional geometries, respectively. Experiments were performed for mass velocities ranging from 100 to 1600 kg m^{-2} s^{-1}, saturation temperatures of 31 and 41°C and vapor qualities from 0.05 to 0.95. The experimental results were compared against the most quoted predictive methods from literature, including the homogeneous

model, methods developed for macro-scale channels and methods specially developed for micro-scale channels. Additionally, a new predictive method was proposed based on the broad experimental database obtained and analyzed in the present study. The new predictive method was not only able to predict accurately the experimental results, but also to capture the main behaviors of the data obtained in the present study and to provide accurate predictions of independent databases from the open literature.

2. *EXPERIMENTAL APPARATUS*

2.1 General description

The experimental setup is comprised of refrigerant and water circuits. The water circuit is intended to condense and subcool the working fluid. The refrigerant circuit is schematically shown in Fig. 1. In the refrigerant circuit, the test fluid is driven by a self-lubricating oil-free micropump through the circuit. The liquid flow rate is set by a frequency inverter acting on the micropump. Downstream the micropump, the mass flow rate is measured with a Coriolis flow meter. Just upstream the pre-heater, the fluid inlet conditions are determined by a thermocouple and an absolute pressure transducer. Downstream the test section, a visualization section, a tube-in-tube heat exchanger, and a refrigerant tank are sequentially located. The heat exchanger is responsible for condensing the vapor created in the heated sections. Additional details of the experimental set up can be found in Tibiriçá and Ribatski (2010) and Sempértegui-Tapia et al. (2013).

2.2 Pre-heater and test section

For the experimental tests in a circular cross-sectional channel, the pre-heater and the test section are formed by a 490 mm horizontal AISI-304 stainless-steel tube,

acquired from *Goofellow Cambridge Limited*, with an OD of 1.47 mm and an ID of 1.1 mm. The arithmetical mean roughness of the circular test section was measured with the optical profiling system Wiko® NT1100 equipment, and a mean average surface roughness (Ra) of 0.289 μm was found based on three measurements along the test section length. Figure 2 shows an image of the inner surface of the test section and the roughness profile obtained through the measurements.

The pre-heater section (diabatic) is 200 mm long and the test section (adiabatic) is 270 mm long. The pre-heater section is heated by applying direct DC current to their surface. The pre-heater and the test section are thermally insulated. The power is supplied to the pre-heater section by a DC power source controlled from the data acquisition system. The pre-heater and the test and visualization sections are connected through junctions made of polyvinylidene fluoride (PVDF) specially designed and machined to match up their ends and keep a smooth and continuous internal surface. Once the fluid has left the test section, its temperature is determined from a 0.25 mm thermocouple whose hot junction is flush-mounted into the pipe wall. The corresponding absolute pressure is estimated from the inlet absolute pressure and the total pressure drop over the pre-heater inlet and the test section outlet given by a differential pressure transducer, Δp. A detailed scheme of the pre-heater and the circular test section is shown in Fig. 3a.

For tests with non-circular channels (see Fig. 3b) a parcel of the length of the test section (190 mm) originally with circular shape was molded into square and triangular shapes. The segments of the test section with triangular and square shapes were obtained through a process of progressive conformation using a steel matrix

composed of two-block with grooves designed especially for each cross section. A uniform compressive stress of approximately 10 tons was provided to the matrix in order to get the desired shape. The inner surface roughness of the test sections were also evaluated after the conformation process. The cross-sectional area of the square and triangular channels were estimated through the image processing of the profiles shown in Fig. 4a and b, respectively, using the software MATLAB R2010a.

Table 2 shows the geometrical characteristics of the test sections evaluated in the present study. This table reveals significant differences of the arithmetic mean roughness of the test sections.

For non-circular channels, the sudden changes of shape from circular into non-circular, and vice versa, are associated to contraction and expansion of the channel cross section. The test sections and the pre-heater are 190 and 200 mm long, respectively. Thermocouples were attached 5 mm downstream the sudden contraction and 5 mm upstream the sudden expansion (necessary distance to minimize the effects of the sudden contraction and expansion on the thermocouples measurements). The thermocouples were fixed tightly against the tube surface. A detailed scheme illustrating the assembly of the non-circular test sections and the pre-heater is shown in Fig. 3b.

2.3 Experimental conditions

Table 3 shows the experimental conditions run in the present study. Experimental tests under conditions of higher mass velocities for R1234ze(E) and R1234yf were not possible due to restrictions imposed to the refrigerant circuit by reduced amount of the fluid available. On the other hand, the mass velocity range for R600a was restricted by the presence of flow instabilities for mass velocities higher than

500 kg/m²s. The vapor quality values shown in Table 3 are the arithmetic average between the vapor quality at the inlet and outlet of the test section (see Eq. (5)), which are practically similar considering that the tests were performed for adiabatic conditions. During the experiments, the saturation temperature was always set at the end of the test section regardless of the cross-sectional geometry.

3. *DATA REDUCTION, EXPERIMENTAL VALIDATION AND UNCERTAINTIES*

3.1 Data reduction

3.1.1 Mass velocity

Mass velocity was calculated as the ratio between the mass flow rate measured by the Coriolis mass flow meter and the internal cross sectional area of the tube, according to the following equation:

$$G = \frac{\dot{M}}{A_{\text{int}}} \tag{1}$$

The cross-sectional area of the circular tube is calculated as follows:

$$A_{\text{int}\,circ} = \frac{\pi D^2}{4} \tag{2}$$

The cross-sectional area of non-circular channels were estimated through the image processing of the test section images illustrated in Fig. 4, as previously mentioned.

3.1.2 Vapor quality

The vapor qualities at the inlet and outlet of the test section were determined through energy balances over the pre-heater and test section according to the following equations, respectively:

$$x_{ts,in} = \frac{1}{i_{LG,ts,in}}\left[\frac{P_{ph}}{\dot{M}} + \left(i_{L,ph,in} - i_{L,ts,in}\right)\right] \quad (3)$$

$$x_{ts,out} = \frac{1}{i_{LG,ts,out}}\left[\frac{P_{ph}}{\dot{M}} + \left(i_{L,ph,in} - i_{L,ts,out}\right)\right] \quad (4)$$

where $i_{L,ph,in}$ is the enthalpy of the liquid at the inlet of the pre-heater, $i_{L,ts,in}$ and $i_{LG,ts,in}$ are the enthalpy of the saturated liquid and the latent heat of vaporization corresponding to the saturation temperature at the inlet of the test section, $T_{ts,in}$, respectively. While, $i_{L,ts,out}$ and $i_{LG,ts,out}$ are the enthalpy of the saturated liquid and the latent heat of vaporization estimated based on the saturation temperature at the outlet of the test section, $T_{ts,out}$, respectively.

The average vapor quality along the test section was estimated as follows:

$$\overline{x}_{ts} = \frac{x_{ts,in} + x_{ts,out}}{2} \quad (5)$$

3.1.3 Single phase frictional pressure drop

Single-phase data were used to validate the pressure drop measurements. Moreover, an accurate estimation of the single-phase pressure drop is mandatory because the data for two-phase frictional pressure drop is obtained by subtracting from the total pressure drop, the parcel corresponding to the single-phase flow length. For the circular geometry, the single-phase frictional pressure drop is directly measured by the differential pressure transducer.

For square and triangular channels, the pressure drop measured by the differential transducer is the sum of the following parcels: the pressure drop along the

circular cross-sectional length of the tube, the pressure drop along the non-circular cross-sectional part of the tube, and the local pressure loss and recovery caused by the sudden contraction and expansion, respectively. Therefore, the total frictional pressure drop over the test section and pre-heater length is given by:

$$\Delta p_{measured} = \Delta p_{f,circ} + \Delta p_{f,ts} + \Delta p_{con} + \Delta p_{\exp} \tag{6}$$

The pressure drop due to the sudden expansion is correlated according to:

$$\Delta p_{\exp} = \Delta p_{\exp,R} + \Delta p_{\exp,I} = \left(\sigma_A^2 - 1 + K_{\exp}\right) \cdot \frac{G^2}{2\rho_L} \tag{7}$$

where K_{exp} is the irreversible loss coefficient given as a function of the expansion area ratio and the momentum correction factor, k:

$$K_{\exp} = 1 - 2k_{ts}\sigma_A + \sigma_A^2\left(2k_c - 1\right) \tag{8}$$

The momentum correction factor for laminar flow is 1.33, 1.377 and 1.41 for circular, triangular and square channel, respectively. These values were estimated using the equation of Rehbock given by Chow (1959):

$$k_{ts} = \frac{\int_0^A v^2 dA}{\overline{v}^2 A} \approx 1 + \frac{\left(v_{\max}/\overline{v} - 1\right)^2}{3} \tag{9}$$

where $v_{\max}/\overline{v}$ are values obtained by Hagen-Pouseuille, Shah and London (1978) and Shah (1975) for circular, square and triangular channels, respectively. For turbulent flow, the momentum correction factor can be approximated to the unity ($k_{ts} \approx k_c \approx 1$) and the Eq. (8) is reduced to the well-known Borda-Carnot correlation.

According to Kays (1950) the pressure drop due to a sudden contraction can be expressed according to:

$$\Delta p_{con} = \left[\frac{1 - \beta_c \sigma_A^2 C_c^2 - 2C_c + 2C_c^2 k_{ts}}{C_c^2}\right] \cdot \frac{G^2}{2\rho_L} \tag{10}$$

where C_c is the area ratio of the vena-contracta and β_c and k_{ts} are the energy and momentum correction factors, respectively. The energy correction factor is equal to 2 for laminar flow and 1 for turbulent flow. The area ratio of the vena-contracta can be estimated using the correlation of Geiger (1964):

$$C_c = 1 - \frac{1-\sigma_A}{2.08\left(1-\sigma_A\right)+0.5371} \tag{11}$$

3.1.4 Two-phase frictional pressure drop

For non-circular channels, the two-phase pressure drop was calculated as the difference of saturation pressures estimated based on the wall temperature measurements from the thermocouples $T_{ts,in}$ and $T_{ts,out}$ located just downstream and just upstream of the inlet and outlet of the test section, respectively, as shown in Fig. 3b. Then, the frictional pressure drop gradient was calculated as the ratio between the two-phase pressure drop minus the accelerational pressure drop and the distance between the thermocouples (L_{ts} = 180 mm), as follows:

$$\left(\frac{dp}{dz}\right)_{f,ts} = \frac{\left[p_{sat}\left(T_{ts,in}\right) - p_{sat}\left(T_{ts,out}\right)\right] - \Delta p_{ac,in-out}}{L_{ts}} \tag{12}$$

where $p_{sat}(T_{ts,in})$ and $p_{sat}(T_{ts,out})$ are the saturation pressures estimated from the temperature measurements and $\Delta P_{ac,in-out}$ is the accelerational pressure drop over the length L_{ts} estimated according to:

$$\Delta p_{ac,in-out} = G^2\left\{\left[\frac{x_{out}^2}{\rho_{G,out}\alpha_{out}} + \frac{\left(1-x_{out}\right)^2}{\rho_{L,out}\left(1-\alpha_{out}\right)}\right] - \left[\frac{x_{in}^2}{\rho_{G,in}\alpha_{in}} + \frac{\left(1-x_{in}\right)^2}{\rho_{L,in}\left(1-\alpha_{in}\right)}\right]\right\} \tag{13}$$

where the subscripts *in* and *out* refer to the positions of the thermocouples $T_{ts,in}$ and $T_{ts,out}$, respectively.

The superficial void fraction was estimated through the method recently proposed by Kanizawa and Ribatski (2015). This new method is based on the principle of minimization of energy dissipation, analogous to the procedure initially proposed by Zivi (Zivi, 1964). This method was chosen because it provided the best estimation of a broad experimental database (more than 3000 data) when compared with previous methods available in the literature. The method of Kanizawa and Ribatski (2015) for horizontal channels is given as follows:

$$\alpha = \left[1 + 1.021 Fr_m^{-0.092} \left(\frac{\mu_L}{\mu_G} \right)^{-0.368} \left(\frac{\rho_G}{\rho_L} \right)^{1/3} \left(\frac{1-x}{x} \right)^{2/3} \right]^{-1} \tag{14}$$

where Fr_m is the Froude number of the mixture, given as follows:

$$Fr_m = \frac{G^2}{(\rho_L - \rho_G)^2 gD} \tag{15}$$

It should be mentioned that the choice of the void fraction prediction method does not have significant impact on the estimation of the two-phase frictional pressure drop for the non-circular channels, because the accelerational pressure drop is almost negligible compared to the frictional pressure drop for an adiabatic test section.

For the circular channel, the frictional pressure drop over the test section length was estimated according to the following equation:

$$\Delta p_{ts} = \Delta p_{measured} - \Delta p_{1\phi} - \Delta p_{2\phi,ph} - \Delta p_{acc,ts} \tag{16}$$

where $\Delta p_{measured}$ is the measured pressure drop by the differential pressure transducer, $\Delta p_{1\phi}$ is the single-phase pressure drop, $\Delta p_{2\phi,ph}$ is the two-phase pressure drop over the pre-heater length and Δp_{acc} is the accelerational pressure drop comprising the adiabatic two-phase flow of the test section.

The single-phase pressure drop $\Delta p_{1\phi}$ is estimated using a single-phase pressure drop correlation and the subcooled region length. The subcooled region length over the

pre-heater was calculated by solving simultaneously energy balance, single-phase pressure drop equations and an equation of state relating the saturation pressure and the saturation temperature from EES.

The two-phase pressure drop along the pre-heater, $\Delta p_{2\phi,ph}$, was estimated through an iterative process as the sum of the pressure drop over 100 discrete elements comprising the beginning of the saturated region at the pre-heater, corresponding the end of the single-phase flow region (*x=0*), and the end of the pre-heater. In this procedure, the transport and thermodynamic properties were calculated locally based on the average saturation pressure of each element. The accelerational and frictional pressure drop parcels along each discrete element were calculated according to Eq. (13) and the predictive method developed in the present study. However, for the first iteration, the method of Müller-Steinhagen and Heck (1986) was adopted to predict the frictional pressure drop parcel. Then, for each iteration a new method for the frictional pressure drop was adjusted and a new value for $\Delta p_{2\phi,ph}$ estimated. This procedure was repeated until the convergence of the solution characterized by a difference between successive values of two-phase pressure drop over the pre-heater lower than 10^{-3} kPa m^{-1} is achieved. The value of Δp_{acc} over the test section was estimated based on Eq. (13) with the subscripts *in* and *out* referring to the position where the two-phase flow begin (x=0) and the end of the pre-heater section. It should be mentioned that the use of a different method to predict the void fraction would mean less than 4% of difference in the estimation of the two-phase pressure drop along the pre-heater, $\Delta p_{2\phi,ph}$.

The pressure drop measurements from the differential transducer were not considered suitable to estimate the frictional pressure for non-circular tests sections due to the presence of singularities (expansion and contraction) along the tube length and

the connections with the differential pressure transducer. In the literature, a reasonable number of methods developed for macro-scale conditions to predict the pressure drop for two-phase flows across sudden expansion and contractions are available. However, as pointed out by Abdelall et al. (2005), Chalfi and Ghiaasiaan (2008) and Chen et al. (2010), they are not recommended for two-phase flows under micro-scale conditions. For this reason, Abdelall et al. (2005), Chen et al. (2010) and more recently Kawahara et al. (2015) developed new methods to predict the pressure drop under micro-scale conditions for expansion and contraction singularities. Their methods are based on experimental data for mixtures of two fluids (water/air, water/N_2, HFE-7200/N_2 and ethanol/N_2). Unfortunately, to the best of the author's knowledge, a method that includes in its database results for halocarbon refrigerants is still not available. It is important to highlight the fact that the surface tension and liquid-gas density ratios of mixtures of non-condensable (air) and water are more than 8 and 15 times higher, respectively, than most of halocarbon refrigerants. Therefore, it is improbable that methods developed to predict two-phase pressure drop along singularities based on data for water/non-condensable gases provide satisfactory predictions of data for halocarbon refrigerants. On the other hand, estimating pressure drop results based on temperature measurements is suitable only for high two-phase flow velocities because small uncertainties of the temperature measurements may imply high uncertainties on the pressure drop estimation for conditions of low pressure drops.

Therefore, the procedure based on the differential pressure drop transducer was used to obtain the data for conditions of low mass velocities corresponding to the tests with the refrigerants R1234ze(E), R1234yf and R600a and the channel with circular geometry (see Table 3). The pressure drop was estimated based on wall temperature measurements for the tests under conditions of high mass velocities corresponding to

the results obtained for the refrigerant R134a and the channels with triangular and square cross-sectional geometries.

In order to check the agreement between both procedures, tests with the refrigerant R134a in a circular channel were also run under conditions of intermediary and high mass velocities. Then, the frictional pressure drop was estimated from wall temperature measurements and from the total pressure drop given by the differential pressure transducer. The differences of frictional pressure drop data estimated according to both procedures were always lower than 5%, hence, within the experimental uncertainty range.

3.2 Experimental validation

3.2.1 Single-phase pressure drop

Experimental tests for single-phase flows were previously performed in order to assure the accuracy of the measurements and evaluate the effective rate of heat losses and consequently the accuracy of vapor quality estimation. The flow is considered as hydrodynamically fully developed at the inlet of the pre-heater section due to the existence of a 100 mm long visualization section upstream the pre-heater, as shown in Fig. 1. Figure 5 illustrates the single-phase pressure drop results for a circular channel. As shown in this figure, the experimental data for laminar flow agree reasonably well with the theory (Hagen-Pouseuille). For turbulent flow, the method of Blasius (1913) provided accurate predictions of the data, resulting a mean absolute error (MAE) of 8.1%.

For non-circular channels, the characteristic length is still an open issue in the area of fluid dynamics and heat transfer. For engineering purposes, the majority of

studies recommends the hydraulic diameter, even though studies for turbulent single-phase flow reported that this procedure overestimates the friction factor for non-circular channels (see Claiborne (1952) and Altemani and Sparrow (1980)). Moreover, it should be taken into account the fact that for regular polygons (equilateral triangle, square channel, etc.); the hydraulic diameter identifies the diameter of the inscribed circle. Therefore, the use of the hydraulic diameter neglects secondary flows and assumes the presence of overstated laminar layers outside the inscribed circle. In order to capture the effect of the cross-sectional dimensions of the channel on the friction factor, Jones Jr. (1976) proposed a modification of the hydraulic diameter by including a factor as a function of the aspect ratio to ensure similarity between the predictions given by circular duct methods with experimental data for rectangular channels. Ahmed and Brundrett (1971) proposed a new characteristic length for regular polygonal channels as the sum of the highest and the lowest isovels, for a square channel $\sqrt{2}a/2$ and $a/2$, respectively, with a being the side length of the channel. Bandopadhayay and Ambrose (1980) also proposed a new generalized characteristic length dimension for non-circular channels, defined as the average distance of the wall channel from the position of maximum velocity. Bahrami et al. (2006) recommended the use of the square root of the channel cross-sectional area, $\sqrt{A}$, as the characteristic length for non-circular channels instead of the hydraulic diameter. Based on this characteristic length, Bahrami et al. (2006) proposed new equations for the analytical solutions for laminar flow considering a Reynolds number having $\sqrt{A}$ as its characteristic length. Duan et al. (2012) also show that the square root of the area, as the length dimension, yields to excellent concordance between experimental data for non-circular channels and the proposed correlations for circular ducts with an easily-done recast using $\sqrt{A}$ as the characteristic length scale. Taking into account this context, it was decided to use the equivalent diameter as the

length dimension, parameter directly related to the square root of the area ($D_{eq} = \sqrt{4A/\pi}$), avoiding the adaptation of the correlation for circular ducts for turbulent flow.

Shah and London (1978) proposed an analytical solution for the friction factor for developed laminar flows inside rectangular channels given as follows:

$$f = \frac{24\left(1 - 1.3553\zeta + 1.9467\zeta^2 - 1.7012\zeta^3 + 0.9564\zeta^4 - 0.2537\zeta^5\right)}{\mathrm{Re}_{Deq}} \cdot \frac{D_{eq}}{D_H} \quad (17)$$

where ζ is the aspect ratio of the rectangular channel and Re_{Deq} is the Reynolds number based on the equivalent diameter.

For equilateral triangular duct with 3 rounded corners, Shah (1975), based on the numerical solution for the friction factor for developed laminar flow, proposed the following equation:

$$f = \frac{15.993}{\mathrm{Re}_{Deq}} \cdot \frac{D_{eq}}{D_H} \quad (18)$$

Figure 6 illustrates the experimental single-phase pressure drop for the refrigerant R134a in a square channel. As shown in this figure, the solution for laminar flow of Shah and London (1978) agrees quite well with the experimental data, providing a mean absolute error lower than 3%. For turbulent flow, the correlations of Blasius (1913) and Petukhov (1970) using the equivalent diameter works relatively well, giving MAEs of 13.1, 15.4 %, respectively.

Figure 7 illustrates the experimental single-phase pressure drop for the refrigerant R134a in a triangular channel. For laminar flow, it can be observed that the correlation presented by Shah (1975) predicts reasonably well the experimental data, providing a mean absolute error lower than 7%. For turbulent flow, the methods of

Blasius (1913) and Petukhov (1970) are able of predicting precisely the experimental data, resulting mean absolute errors lower than 8%. The flow was considered to be fully developed since there is more than $250D$ between the inlet of the preheater and the beginning of the non-circular test section. It is important highlighting that the sum of the pressure drop due to the test section contraction and the pressure recovery due to the test section expansion varies from 0.04 to 3.4% of the total pressure drop for non-circular channels. Therefore, their estimation could have been neglected.

As observed, for turbulent flow, the single-phase pressure drop correlations developed for circular channels works accurately for the experimental data for the 4 working fluids (R134a, R1234ze(E), R1234yf and R600a) and also for the non-circular tests using the equivalent diameter as the characteristic dimension. For laminar flow in non-circular channels, the adaptation to the laminar theory as indicated in Eqs. (17) and (18) also provided reasonable predictions.

3.2.2 Single-phase heat transfer coefficient

Heat transfer coefficients for single-phase flows are also analyzed here in order of validating energy balances along the pre-heater and the test sections. The single-phase heat transfer coefficient was estimated using the last thermocouple in order to get a thermally fully developed condition. Figure 8 illustrates a comparison of experimental and estimated values for single-phase heat transfer coefficients. As noted in this figure, the correlation for laminar, thermally developing flow of Siegel et al. (1958), Chandrupatla and Sastri (1977) and Wibulswas (1966) capture adequately the experimental data for circular, square and triangular channels, respectively. However, these correlations underestimate the experimental values in around 20%. For turbulent flow, the correlation of Gnielinski (1976) agrees quite well with the experimental values

for circular channel, independently of the refrigerant. For the square channel, the correlation of Gnielinski (1976) also predicts reasonably well the experimental values, however, for the triangular channel the correlation under predicts the experimental data especially for high Reynolds number. It can also be observed that the experimental transition from laminar to turbulent flow seems to occur for a Reynolds number between 2000 and 2500 approximately that agrees with the theory.

3.3 Uncertainties analysis

Temperature measurements were calibrated and the temperature uncertainty was evaluated according to the procedure suggested by Abernethy et al.(1973). Accounting for all instrument errors, uncertainties for the calculated parameter were estimated using the method of sequential perturbation according to Taylor and Kuyatt (1994). All the experimental uncertainties associated with the sensors and calculated parameters are listed in Table 4.

4. *EXPERIMENTAL RESULTS*

4.1 Two-phase frictional pressure drop

As qualitative general behavior, the pressure drop increases with increasing the vapor quality until a maximum value is attained at high vapor qualities. After this pressure drop peak, further increments of vapor quality result in a pressure drop decrease. The vapor quality corresponding to the peak varies according to the channel geometry, fluid, saturation temperature, and channel characteristic dimension, as pointed out by Ribatski (2014).

4.1.1 Effect of working fluid

Figure 9 illustrates the effect of the working fluid on the two-phase pressure drop gradient. As observed, the pressure drop gradient is higher for R600a when compared with R1234ze(E), R1234yf and R134a. This behavior is explained by the fact that the specific volume of the gas phase for R600a is about 3 to 4.5 times higher than for the other fluids. This implies much higher superficial velocity of the two-phase mixture for R600a, and, consequently, higher pressure drop gradients. According to Fig. 9a, the pressure drop gradient of R134a and R1234yf are almost similar, except for high vapor qualities where the pressure drop gradient for the fluid R134a is slightly higher. It can also be observed that the pressure drop gradient of R1234ze(E) is approximately 25% higher when compared to the pressure drop gradient of R134a. The pressure drop peak for R600a seems to occur for lower vapor qualities compared to the other fluids.

4.1.2 Effect of saturation temperature

Figure 10 illustrates the effect of saturation temperature on the frictional pressure drop gradient during adiabatic flow. As expected, the frictional pressure drop decreases with increasing saturation temperature from 31°C to 41°C for R134a. The same effect of the saturation temperature on the pressure drop was verified for R600a in a circular channel (Fig. 10b). The vapor quality corresponding to the pressure drop peak is shifted to lower vapor qualities with decreasing the saturation temperature. This behavior is intensified for R600a.

4.1.3 Effect of mass velocity

Figure 11 illustrates the effect of the mass velocity on the two-phase pressure drop gradient. As observed in this figure, the pressure drop increases with increasing the mass velocity. An analysis of the experimental data for circular and square channels (Fig. 11a and 11b) reveals that the pressure gradient peak moves to lower vapor qualities with increasing mass velocity. This behavior seems to be negligible according to the experimental data for triangular channel shown in Fig. 11c.

4.1.4 Effect of the cross-sectional geometry

Figure 12a illustrates the effect of the cross-sectional geometry on the two-phase pressure drop gradient for the channels evaluated in the present study. Figure 12b shows for two different mass velocities the variation with vapor quality of the ratio of pressure drop for non-circular and circular channels under the same experimental conditions. The highest pressure drop gradients are observed for the triangular geometry. The square channel also provides pressure drop gradients higher than the circular channel. This result is partially explained by the size of the equivalent diameters that increases according to the following order of geometries: triangular, square and circular.

In general, according to Fig. 12b, the ratio $(dp/dz)_{non\text{-}circ}/(dp/dz)_{circ}$ decreases with increasing mass velocity, passing through a minimum value at a vapor quality close to 0.7. Curiously, the ratio $(dp/dz)_{non\text{-}circ}/(dp/dz)_{circ}$ is affected, by a variation of 100% in the mass velocity, only marginally for most of the vapor quality range.

4.2 Assessment of predictive methods

Table 5 provides the mean absolute error (MAE) and the parcel of data predicted within an error band of ±20 % (η) obtained from comparisons between eleven methods from literature and the experimental database gathered in the present study. Results of comparisons are presented for the overall database and for each dataset characterized by the pair: channel geometry and fluid refrigerant. The predictive methods were evaluated using the characteristic dimension recommended by the original authors. For the methods that do not specify the characteristic dimension and were developed based only on results for circular channels, the equivalent diameter was used based on the discussion presented in the Section 3.2. The predictive methods presented in Table 5 were considered based on the following criteria: (i) the most quoted predictive methods in the literature; (ii) predictive methods based on broad experimental databases, iii) updated versions of well-known predictions methods, i.e. Zhang et al. (2010) instead of Mishima and Hibiki (1996) or Del Col et al. (2013) instead of Cavallini et al. (2009).

For the comparisons involving the overall database, the method of Müller-Steinhagen and Heck (1986), Del Col et al. (2013) and Friedel (1979) provided the best results, predicting more than 55% of the experimental data within an error band of ±20%. The methods of Sun and Mishima (2009) and Kim and Mudawar (2012) provided predictions with almost the same accuracy, giving a mean absolute error of 19.6%. The homogenous model using the two-phase viscosity according to Cicchitti et al. (1960) performed relatively well providing a MAE of approximately 20%. The methods of Muller-Steinhagen and Heck (1986), Kim and Mudawar (2012) and Sun and Mishima (2009) were also indicated as the best by Kim and Mudawar (2014), based on a comparison against a broad database containing more than 7000 experimental results gathered in the literature. The homogeneous model with the two-phase viscosity given by Dukler et al. (1964), the methods by Lockhart and Martinelli (1949), Zhang et al. (2010), Li and Wu (2011) and the phenomenological method proposed by Cioncolini et al. (2009) provided MAE values higher than 30% and η lower than 40%.

The homogeneous model with the two-phase viscosity given by Cicchitti et al. (1960) provided accurate predictions of the experimental results for R134a, independently of the channel geometry. This result is not surprising, because several authors have reported that the homogeneous model with the two-phase viscosity given by Cicchitti et al. (1960) provides reasonable predictions of their respective databases mostly comprised by experimental data for R134a (see Ribatski et al. (2006) and Felcar and Ribatski (2008)). On the other hand, Cicchitti et al. (1960) was not satisfactory for the low GWP refrigerants (R1234ze(E) and R1234yf) and the isobutane (R600a), predicting less than 20% within an error band of ±20%.

The method of Müller-Steinhagen and Heck (1986) provided accurate predictions of the circular and square databases for refrigerant R134a. The experimental

results for circular channel and the fluids R1234ze(E) and R600a are also satisfactorily predicted by this method. On the other hand, the method of Müller-Steinhagen and Heck (Müller-Steinhagen and Heck, 1986) failed to predict the experimental data for triangular channel/R134a and R1234yf, providing mean absolute errors of 26.1 and 21.9 %, respectively.

The methods of Friedel (1979) and Del Col et al. (2013) provided relatively accurate results for circular and square channels with R134a, but failed to predict the data for triangular channel and the experimental dataset for the fluid R1234yf. It is worth to mention that the method of Del Col et al. (2013) was developed for small diameter channels and takes into account the relative roughness of the channel. The method of Del Col et al. (2013) was developed based on the correlation proposed by Friedel (1979) for conventional channels. Therefore, it is not surprising that both methods provided almost similar predictions for the R134a. However, the method by Del Col et al. (2013) improves substantially the predictions given by Friedel (1979) for R1234ze(E) and R600a, providing η values higher than 80%.

The methods of Sun and Mishima (2009) and Kim and Mudawar (2012) works relatively well for the experimental data of R134a, providing MAE values lower than 20% regardless of the cross-sectional geometry. However, both methods failed to predict the experimental data for R1234ze(E), R1234yf and R600a. This result could be explained by the fact that neither Sun and Mishima (2009) nor Kim and Mudawar (2012) included these fluids in the experimental database used to develop their methods.

It can be noted in Table 5 that the method developed by Zhang et al. (2010) does not provide reasonable predictions of the experimental database, regardless of the working fluid and cross-sectional geometry. This result is probably explained by the fact that the method is not recommended for both phases being turbulent and 34% of the

experimental data obtained in the present study are for conditions with both phases as turbulent. The phenomenological model developed by Cioncolini et al. (2009) for annular flow pattern also failed to predict the experimental database, providing mean absolute errors higher than 33%. The homogeneous model with the two-phase viscosity given by Dukler et al. (1964), the methods by Lockhart and Martinelli (1949) and Li and Wu (2011) were not able of providing reasonable predictions of the datasets acquired in the present study.

Figure 13 illustrates comparisons between the experimental database segregated according to the working fluid and the methods developed by Müller-Steinhagen and Heck (1986), Kim and Mudawar (2012), Del Col et al. (2013) and Sun e Mishima (2009). According to this figure, the four methods mostly underestimate the experimental data for R1234ze(E), R1234yf and R600a, while overestimate the experimental data for R134a. It should also be highlighted the fact that these four methods work better for pressure drop gradient ranging from 60 to 300 kPa m^{-1}.

Due to the fact that a predictive method should be not only statistically accurate, but also be able of capturing the main trends of the experimental results, Figure 14 and 15 display the evolution of the two-phase pressure drop gradient with the vapor quality according to the predictive methods from literature and the experimental data obtained for non-circular and circular channels, respectively. According to Figure 14a, for the experimental data for R134a in the square channel, Sun and Mishima (2009) and the homogeneous model with the two-phase viscosity given by Cicchitti et al. (1960) capture reasonably well the trend of the experimental pressure drop. The methods developed by Friedel (1979), Müller-Steinhagen and Heck (1986), Kim and Mudawar (2012) and Del Col et al. (2013) work well for low vapor qualities. For the triangular

channel (see Fig. 14b and 14c), Sun and Mishima (2009), the homogeneous model with the two-phase viscosity given by Cicchitti et al. (1960) and Müller-Steinhagen and Heck (1986) capture reasonably well the trend of the experimental pressure drop gradient regardless of the mass velocity.

According to Fig. 15a, for R1234ze(E), the methods of Friedel (1979), Del Col et al. (2013) and Müller-Steinhagen and Heck (1986) capture the experimental trends relatively well. For R1234yf, Friedel (1979) and Müller-Steinhagen and Heck (1986) capture relatively well the trend of the experimental pressure drop. As observed in Fig. 15c, the method developed by Del Col et al. (2013) provides reasonable predictions of the experimental trends for the refrigerant R600a.

Despite being statistically the most accurate predictive methods for the overall database, Müller-Steinhagen and Heck (1986) and Friedel (1979) were not able to capture the trends of experimental results for several experimental conditions. As previously discussed, Sun and Mishima (2009) and the homogeneous model with the two-phase viscosity given by Cicchitti et al. (1960) were able to capture the trends of the experimental data for R134a, and Müller-Steinhagen and Heck (1986), Friedel (1979) and Del Col et al. (2013) capture the pressure drop trends observed for R1234ze(E), R1234yf and R600a.

5. *DEVELOPMENT OF A NEW PREDICTIVE METHOD*

5.1 Description of the new predictive method

Due to the fact that none of the predictive methods from literature was able to predict accurately the experimental data for all range of conditions evaluated in the present study, in this item a new predictive method is proposed. Adopting similar approach implemented by Da Silva and Ribatski (2013), the new predictive method is based on the proposal of Müller-Steinhagen and Heck (1986) because of its simplicity and reasonable capability of providing reasonable predictions of independent experimental databases available in the literature.

The method by Müller-Steinhagen and Heck (1986) is given according to:

$$\left(\frac{dp}{dz}\right)_{2\phi} = F \cdot (1-x)^{1/\lambda} + \left(\frac{dp}{dz}\right)_{G0} \cdot x^{\lambda} \tag{19}$$

$$F = \left(\frac{dp}{dz}\right)_{L0} + \omega \cdot \left[\left(\frac{dp}{dz}\right)_{G0} - \left(\frac{dp}{dz}\right)_{L0}\right] \cdot x \tag{20}$$

where the coefficients ω and λ are equal to 2 and 3, respectively. This method was developed based on 9313 experimental data for circular conventional channels (tube diameters larger than 3 mm). Therefore, it is important to highlight the fact that the accuracy of the method of Müller-Steinhagen and Heck (1986) can be improved for the experimental conditions considered in the present study including circular and non-circular small diameter channels. Moreover, the present database includes results for new refrigerants (R1234ze(E), R1234yf and R600a). These fluids are not considered in the database of Müller-Steinhagen and Heck (1986). Additionally, the new method was developed considering a coherent approach by adopting a unique characteristic dimension during the data regression procedure and during the adjustment of its empirical constants.

Initially, values of ω and λ in Eqs. (19) and (20) were obtained for each set of mass velocity condition by a regression analysis through the least squares fitting method. By analyzing those values, it was found that ω decreases with increasing the mass velocity, while the effect of mass velocity on λ was found almost negligible regardless of the experimental condition. Based on these results, the exponent λ was assumed constant and the exponent ω a function of the mass velocity. Several fitting equation forms were evaluated in order to predict the exponent ω as a function of G. The best predictions of exponent ω were provided by the following relationship:

$$\omega = a \cdot e^{b \cdot \mathrm{Re}_{Go}/1000} \tag{21}$$

where the Reynolds number is calculated with the equivalent diameter as the characteristic dimension for non-circular channels. The coefficients a, b and λ were adjusted using the least square method for non-linear equations given by the software MATLAB R2015a. Through this procedure, values of a, b and λ equal to 3.01, -0.00464 and 2.31 were found, respectively. Table 6 summarizes the process of implementation of the new method proposed in the present study.

5.2 Evaluation of the proposed method

Table 7 lists the mean absolute error, mean relative error and the parcel of data predicted within error bands of ±30% and ±20% obtained from the comparisons between the experimental database and the new predictive method. As observed in this table, for the overall database, the proposed method predicted 97.2% and 89.2 % of the experimental data within error bands of ±30% and ±20%, respectively. The new method also provides accurate predictions of the particular datasets regardless of the fluid and the cross-sectional geometry, providing values of MAE lower than 12% and $\eta_{20\%}$ higher than 80%.

Figure 16 illustrates a comparison between the experimental results and the predictions given by the new method. According to this figure, the new method is accurate, independently of the pressure gradient range and the working fluid.

Figure 17 depicts the parcel of the experimental data predicted within an error band of ±20% according to the methods of Müller-Steinhagen and Heck (1986), Kim and Mudawar (2012), Del Col et al. (2013) and the new predictive method. In this figure, comparisons are performed for the data segregated according to ranges of vapor quality and mass velocity. As shown in Fig. 17a for the methods from literature, the parcel of data predicted within an error band of ±20% does not vary significantly according to the vapor quality range, presenting values between 40 and 60%. On the other hand, the method proposed in the present study predicts more than 80% of the experimental data within the same error band for vapor qualities higher than 0.2. For vapor qualities lower than 0.2, the new method also over performed the methods from

literature providing a value of $\eta_{20\%}$ higher than 65%. According to Fig. 17b, the method proposed in the present study also provides better predictions than the methods from literature independent of the mass velocity range.

As shown in Fig. 18, the new method is able to capture the effects on the pressure drop of mass velocity, saturation temperature, working fluid and equivalent diameter. Moreover, the method also predicts satisfactorily the experimental trends for the four fluids and 3 cross-sectional geometries evaluated in the present study.

In order to check the accuracy of the new method against independent databases from literature, experimental data were gathered from the studies of Del Col et al.(2013), Ducoulombier et al. (2011), Del Col et al. (2015) and Del Col et al. (2014) and compared with the predictions provided by the present method.

According to Table 8, the new predictive method satisfactorily predicts the experimental results of the independent database, providing an overall mean absolute error of only 12.7%. It is important to highlight the fact that the new method provides satisfactory predictions of the results of the fluids CO_2 and propane, which are fluids not included in the database used for the adjustment of the new method.

6. *CONCLUSIONS*

The following remarks summarize the conclusions of the present investigation:

- A broad experimental database for two-phase frictional pressure drop in a single micro-scale channel was obtained. The experimental database comprises 1468 experimental data points and covers 4 working fluids (R134a, R1234ze(E), R1234yf

and R600a), three cross-sectional geometries (circular, square and triangular sections), mass velocities from 100 to 1600 kg $m^{-2}s^{-1}$, saturation temperatures of 31 and 41°C, vapor qualities from 0 to 0.95 and internal equivalent diameters of 1.1, 0.977 and 0.835 mm.

- An analysis concerning the characteristic dimension for non-circular channels was performed. Based on this analysis, it was addressed that although the hydraulic diameter is frequently applied, its use is questionable. Furthermore, it was verified experimentally that the correlations for single-phase frictional pressure drop in turbulent flow for a circular channel also worked for non-circular channels when the equivalent diameter was used as the characteristic dimension.
- From a parametric analysis of the experimental results, it can be concluded that the two-phase frictional pressure drop for R600a is higher compared to the other fluids. Moreover, the two-phase frictional pressure drop gradient of R1234ze(E) is higher than of R134a and R1234yf, which happen to be almost similar except under high vapor quality conditions.
- The two-phase frictional pressure gradient increases with increasing mass velocity. The frictional pressure drop gradient presents a peak, which moves to lower vapor qualities with increasing mass velocities for square and circular channels. The frictional pressure drop gradient decreases with increasing saturation temperature. Highest pressure drop gradients were observed for the triangular channel followed by square and circular geometries. This result is partially explained by the size of the equivalent diameters.
- The methods of Del Col et al. (2013), Müller-Steinhagen and Heck (1986), Friedel (1979), Sun and Mishima (2009) and Kim and Mudawar (2012) provided relatively

reasonable predictions of the experimental database. However, they failed to predict particular datasets characterized by the pair fluid refrigerant and channel geometry.

- A new predictive method based on Müller-Steinhagen and Heck (2012) was proposed. This method provided accurate predictions of the experimental database used for its development, predicting 97.1% and 89.2% of the data within error bands of ±30 and ±20%, respectively. The proposed method also provided satisfactory predictions of independent experimental results presented by Ducoulombier et al. (2011), Del Col et al. (2015) and Del Col et al. (2014) for the fluids CO_2, R1234ze(E) and propane, respectively.

7. *ACKNOWLEDGEMENTS*

The authors gratefully acknowledge FAPESP (The State of São Paulo Research Foundation, Brazil) for the financial support under contract numbers 2010/17605-4 and 2011/50176-2 and CNPq (The National Council for Scientific and Technological Development, Brazil) for the financial support under Contract Numbers nº476763/2013-4 and 303852/2013-5. The technical support given to this investigation by Mr. José Roberto Bogni is also appreciated and deeply recognized. The authors also thank Prof. Renato Goulart Jasinevicius for the support in obtaining the profiles of the test sections and measuring the surface roughness. The authors are also grateful to Honeywell for supplying the low GWP refrigerants R1234ze(E) and R1234yf.

8. *REFERENCES*

Abdelall, F.F., Hahn, G., Ghiaasiaan, S.M., Abdel-Khalik, S.I., Jeter, S.S., Yoda, M., Sadowski, D.L., 2005. Pressure drop caused by abrupt flow area changes in small channels. Exp. Therm. Fluid Sci. 29, 425–434. doi:10.1016/j.expthermflusci.2004.05.001

Abernethy, R.B., Powell, B.D., Colbert, D.L., Sanders, D.G., Thompson Jr, J.W., 1973. Handbook uncertainty in gas turbine measurements, Arnold Eng. ed. Tennessee.

Ahmed, S., Brundrett, E., 1971. Characteristic lenght for non-circular ducts. Int. J. Heat Mass Transf. 14, 157–159.

Altemani, C.A.C., Sparrow, E.M., 1980. Turbulent Heat Transfer and Fluid Flow in an Unsymmetrically Heated Triangular Duct. J. Heat Transfer 102, 590–597.

Bahrami, M., Yovanovich, M.M., Culham, J.R., 2006. Pressure Drop of Fully-Developed, Laminar Flow in Microchannels of Arbitrary Cross-Section. J. Fluids Eng. 128, 1036. doi:10.1115/1.2234786

Bandopadhayay, P.C., Ambrose, C.W., 1980. A generalised lenght dimension for non-circular ducts. Lett. Heat Mass Transf. 7, 323–328.

Beattie, D.R.H., Whalley, P.B., 1982. A simple two-phase frictional pressure drop calculation method. Int. J. Multiph. Flow 8, 83–87.

Blasius, H., 1913. Das ahnlichkeitsgesetz bei reibungsvorg/ingen in fltissigkeiten. Forschg. Arb. Ing. Wes. 131.

Calm, J.M., 2008. The next generation of refrigerants - Historical review, considerations, and outlook. Int. J. Refrig. 31, 1123–1133. doi:10.1016/j.ijrefrig.2008.01.013

Cavallini, A., Del Col, D., Matkovic, M., Rossetto, L., 2009. Frictional pressure drop during vapour–liquid flow in minichannels: Modelling and experimental evaluation. Int. J. Heat Fluid Flow 30, 131–139. doi:10.1016/j.ijheatfluidflow.2008.09.003

Chalfi, T.Y., Ghiaasiaan, S.M., 2008. Pressure drop caused by flow area changes in capillaries under low flow conditions. Int. J. Multiph. Flow 34, 2–12. doi:10.1016/j.ijmultiphaseflow.2007.09.004

Chandrupatla, A.R., Sastri, V.M.K., 1977. Laminar forced convection heat transfer of a non-newtonian fluid in a square duct. Int. J. Heat Mass Transf. 20, 1315–1324. doi:10.1016/0017-9310(77)90027-8

Chen, I.Y., Wongwises, S., Yang, B.-C., Wang, C.-C., 2010. Two-Phase Flow Across Small Sudden Expansions and Contractions. Heat Transf. Eng. 31, 298–309. doi:10.1080/01457630903312056

Chow, V. Te, 1959. Open-channel hydraulics. McGraw-Hill B. Co. doi:ISBN 07-010776-9

Cicchitti, A., Lombardi, C., Silvestri, M., 1960. Two-phase cooling experiments: pressure drop, heat transfer and burnout measurements. Energ. Nucl. 7, 417–425.

Cioncolini, A., Thome, J.R., Lombardi, C., 2009. Unified macro-to-microscale method to predict two-phase frictional pressure drops of annular flows. Int. J. Multiph. Flow 35, 1138–1148. doi:10.1016/j.ijmultiphaseflow.2009.07.005

Claiborne, H.C., 1952. A critical review of the literature on pressure drop in noncircular ducts and annuli. Technical Information Service, Oak Ridge National Laboratory, Oak Ridge, Tennessee.

Da Silva, J.D., Ribatski, G., 2013. Two-phase frictional pressure drop of halocarbon refrigerants inside small diameter tubes: data analysis and the proposition of a new frictional pressure drop correlation, in: 8th International Conference on Multiphase Flow. Jeju-Korea.

Del Col, D., Bisetto, A., Bortolato, M., Torresin, D., Rossetto, L., 2013. Experiments and updated model for two phase frictional pressure drop inside minichannels. Int. J. Heat Mass Transf. 67, 326–337. doi:10.1016/j.ijheatmasstransfer.2013.07.093

Del Col, D., Bortolato, M., Azzolin, M., Bortolin, S., 2015. Condensation heat transfer and two-phase frictional pressure drop in a single minichannel with R1234ze(E) and other refrigerants. Int. J. Refrig. 50, 87–103. doi:10.1016/j.ijrefrig.2014.10.022

Del Col, D., Bortolato, M., Bortolin, S., 2014. Comprehensive experimental investigation of two-phase heat transfer and pressure drop with propane in a minichannel. Int. J. Refrig. 47, 66–84. doi:10.1016/j.ijrefrig.2014.08.002

Duan, Z., Yovanovich, M.M., Muzychka, Y.S., 2012. Pressure Drop for Fully Developed Turbulent Flow in Circular and Noncircular Ducts. J. Fluids Eng. 134, 061201. doi:10.1115/1.4006861

Ducoulombier, M., Colasson, S., Bonjour, J., Haberschill, P., 2011. Carbon dioxide flow boiling in a single microchannel – Part I: Pressure drops. Exp. Therm. Fluid Sci. 35, 581–596. doi:10.1016/j.expthermflusci.2010.12.010

Dukler, A.E., Wicks, M., Cleaveland, R.G., 1964. Pressure drop and hold up in two-phase flow. AIChE J. 10, 38–51.

Felcar, H.O.M., Ribatski, G., 2008. Avaliação de métodos preditivos para perda de carga durante o escoamento bifásico e a ebulição convectiva em micro-canais, in: 1° Encontro Brasileiro Sobre Ebulição, Condensação E Escoamento Multifásico Líquido-Gás. Florianópolis.

Friedel, L., 1979. Pressure drop during gas/vapor-liquid flow pipes. Int. Chem. Eng.

Geiger, G.E., 1964. Sudden contraction losses in single and two-phase flow. PhD Thesis, University of Pittsburg, Pittsburg, PA.

Gnielinski, V., 1976. New equations for heat and mass transfer in turbulent flow in pipes and channels. Int. Chem. Eng. 359–368.

Huang, H., Borhani, N., Thome, J.R., 2016. Experimental investigation on flow boiling pressure drop and heat transfer of R1233zd(E) in a multi-microchannel evaporator. Int.

J. Heat Mass Transf. 98, 596–610. doi:http://dx.doi.org/10.1016/j.ijheatmasstransfer.2016.03.051

Jones Jr., O.C., 1976. An Improvement in the Calculation of Turbulent Friction in Rectangular Ducts. J. Fluids Eng.

Kanizawa, F.T., Ribatski, G., 2015. A new void fraction predictive method based on the minimum energy dissipation. J. Braz. Soc. Mech. Sci. Eng. doi:10.1007/s40430-015-0446-x

Kawahara, A., Mansour, M.H., Sadatomi, M., Law, W.Z., Kurihara, H., Kusumaningsih, H., 2015. Characteristics of gas–liquid two-phase flows through a sudden contraction in rectangular microchannels. Exp. Therm. Fluid Sci. 66, 243–253. doi:10.1016/j.expthermflusci.2015.03.030

Kays, W.M., 1950. Loss Coefficients for Abrupt Changes in Flow Cross Section with Low Reynolds Number Flow in Single and Multiple Tube Systems. Stanford University. Dept. of Mechanical Engineering, Navy, United States.

Kim, S.-M., Mudawar, I., 2014. Review of databases and predictive methods for pressure drop in adiabatic, condensing and boiling mini/micro-channel flows. Int. J. Heat Mass Transf. 77, 74–97. doi:http://dx.doi.org/10.1016/j.ijheatmasstransfer.2014.04.035

Kim, S.-M., Mudawar, I., 2012. Universal approach to predicting two-phase frictional pressure drop for adiabatic and condensing mini/micro-channel flows. Int. J. Heat Mass Transf. 55, 3246–3261. doi:10.1016/j.ijheatmasstransfer.2012.02.047

Li, W., Wu, Z., 2011. Generalized adiabatic pressure drop correlations in evaporative micro/mini-channels. Exp. Therm. Fluid Sci. 35, 866–872. doi:10.1016/j.expthermflusci.2010.07.005

Lockhart, R.W., Martinelli, R.C., 1949. Proposed correlation of data for isothermal two-phase two component flow in pipes. Chem. Eng. Prog. 45, 39.

Mishima, K., Hibiki, T., 1996. Some characteristics of air-water two-phase flow in small diameter vertical tubes. Int. J. Multiph. Flow.

Mota-Babiloni, A., Navarro-Esbrí, J., Barragán, Á., Molés, F., Peris, B., 2014. Drop-in energy performance evaluation of R1234yf and R1234ze(E) in a vapor compression system as R134a replacements. Appl. Therm. Eng. 71, 259–265. doi:10.1016/j.applthermaleng.2014.06.056

Müller-Steinhagen, H., Heck, K., 1986. A simple friction pressure drop correlation for two-phase flow in pipes. Chem. Eng. Process. Process Intensif. 20, 297–308. doi:10.1016/0255-2701(86)80008-3

Pamitran, A.S., Choi, K.I., Oh, J.T., Hrnjak, P., 2010. Characteristics of two-phase flow pattern transitions and pressure drop of five refrigerants in horizontal circular small tubes. Int. J. Refrig. 33, 578–588. doi:10.1016/j.ijrefrig.2009.12.009

Petukhov, B.S., 1970. Heat Transfer and Friction in Turbulent Pipe Flow with Variable Physical Properties, in: Transfer, J.P.H. and T.F.I.B.T.-A. in H. (Ed.), . Elsevier, pp. 503–564. doi:http://dx.doi.org/10.1016/S0065-2717(08)70153-9

Ribatski, G., 2014. Estudo da ebulição convectiva no interior de canais de dimensões reduzidas. Thesis Livre Docencia, University of São Paulo.

Ribatski, G., 2013. A Critical Overview on the Recent Literature Concerning Flow Boiling and Two-Phase Flows Inside Micro-Scale Channels. Exp. Heat Transf. 26, 198–246. doi:10.1080/08916152.2012.737189

Ribatski, G., Wojtan, L., Thome, J.R., 2006. An analysis of experimental data and prediction methods for two-phase frictional pressure drop and flow boiling heat transfer

in micro-scale channels. Exp. Therm. Fluid Sci. 31, 1–19. doi:10.1016/j.expthermflusci.2006.01.006

Ribatski, G., Zhang, W., Consolini, L., Xu, J., Thome, J.R., 2007. On the Prediction of Heat Transfer in Micro-Scale Flow Boiling. Heat Transf. Eng. 28, 842–851. doi:10.1080/01457630701378267

Sempértegui-Tapia, D., De Oliveira Alves, J., Ribatski, G., 2013. Two-Phase flow characteristics during convective boiling of halocarbon refrigerants inside horizontal small-diameter tubes. Heat Transf. Eng. 34, 1073–1087. doi:10.1080/01457632.2013.763543

Shah, R.K., 1975. Laminar flow friction and forced convection heat transfer in ducts of arbitrary geometry. Int. J. Heat Mass Transf. 18, 849–862. doi:10.1016/0017-9310(75)90176-3

Shah, R.K., London, A.L., 1978. Laminar flow forced convection in ducts. Adv. Heat Transfer Supplement 1, Academic P. ed. New York.

Siegel, R., Sparrow, E.M., Hallman, T.M., 1958. Steady laminar heat transfer in a circular tube with prescribed wall heat flux. Appl. Sci. Res. Sect. A 7, 386–392. doi:10.1007/BF03184999

Sun, L., Mishima, K., 2009. Evaluation analysis of prediction methods for two-phase flow pressure drop in mini-channels. Int. J. Multiph. Flow 35, 47–54. doi:10.1016/j.ijmultiphaseflow.2008.08.003

Taylor, B.N., Kuyatt, C.E., 1994. Guidelines for Evaluating and Expressing the Uncertainty of NIST Measurement Results. NIST Tech. Note 25.

Tibiriçá, C.B., Ribatski, G., 2013. Flow boiling in micro-scale channels – Synthesized literature review. Int. J. Refrig. 36, 301–324. doi:10.1016/j.ijrefrig.2012.11.019

Tibiriçá, C.B., Ribatski, G., 2010. Flow boiling heat transfer of R134a and R245fa in a 2.3mm tube. Int. J. Heat Mass Transf. 53, 2459–2468. doi:10.1016/j.ijheatmasstransfer.2010.01.038

Wibulswas, P., 1966. Laminar-flow heat transfer in non-circular ducts. PhD Thesis, University College London. doi:10.1115/1.1845554

Wu, J., Koettig, T., Franke, C., Helmer, D., Eisel, T., Haug, F., Bremer, J., 2011. Investigation of heat transfer and pressure drop of CO2 two-phase flow in a horizontal minichannel. Int. J. Heat Mass Transf. 54, 2154–2162. doi:10.1016/j.ijheatmasstransfer.2010.12.009

Zhang, W., Hibiki, T., Mishima, K., 2010. International Journal of Heat and Mass Transfer Correlations of two-phase frictional pressure drop and void fraction in mini-channel. Int. J. Heat Mass Transf. 53, 453–465. doi:10.1016/j.ijheatmasstransfer.2009.09.011

Zivi, S.M., 1964. Estimation of Steady-State Steam Void-Fraction by Means of the Principle of Minimum Entropy Production. J. Heat Transfer 86.

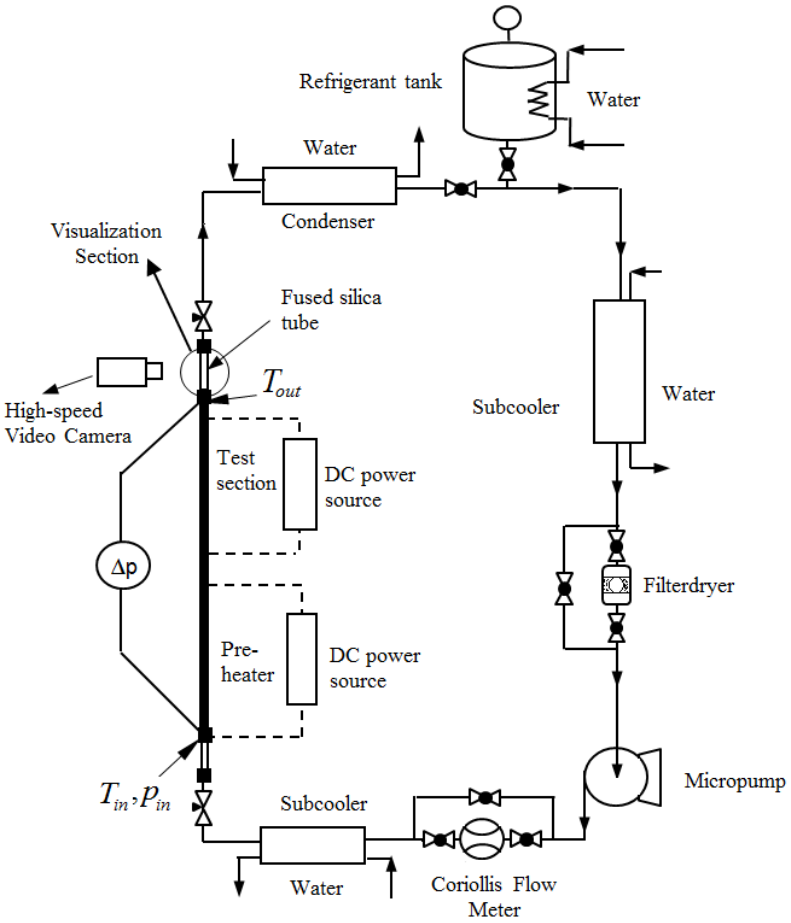

Figure 1. Esquematic diagram of the refrigerant circuit.

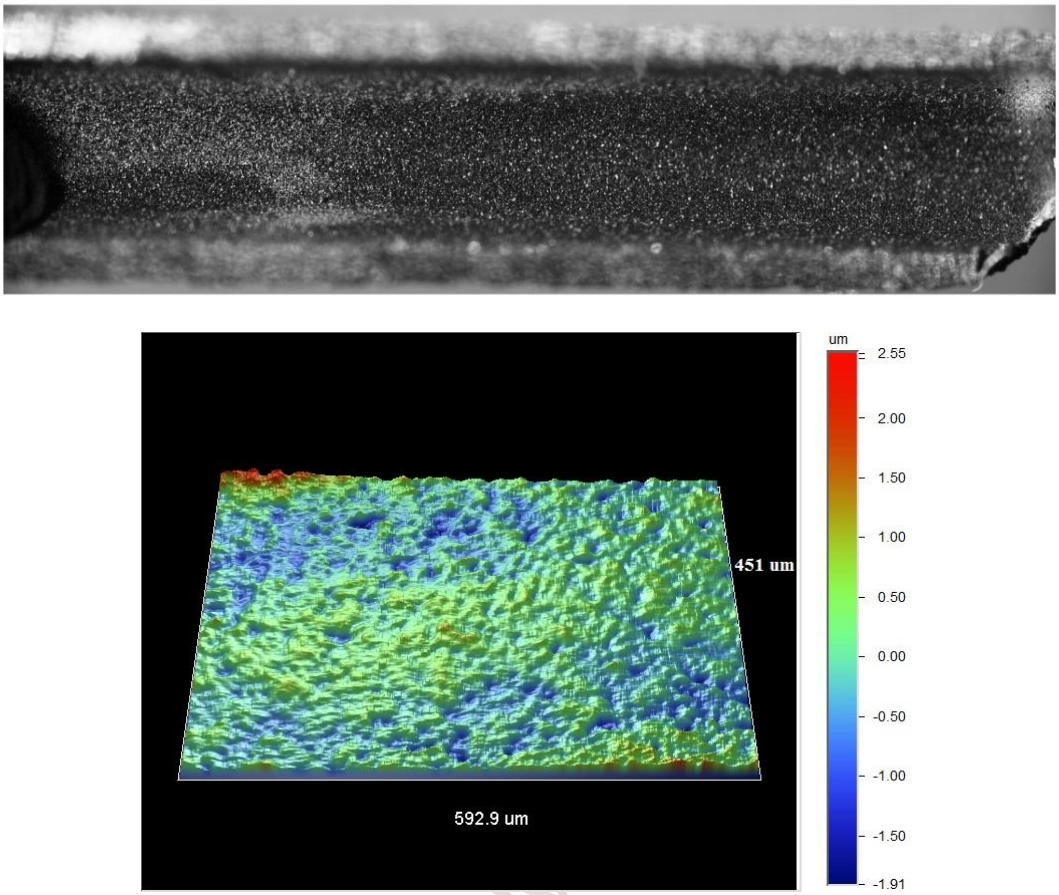

Figure 2. a) Image of the inner surface of the channel, b) 3D image of the microchannel inner surface taken by the optical profiling system Wiko® NT110.

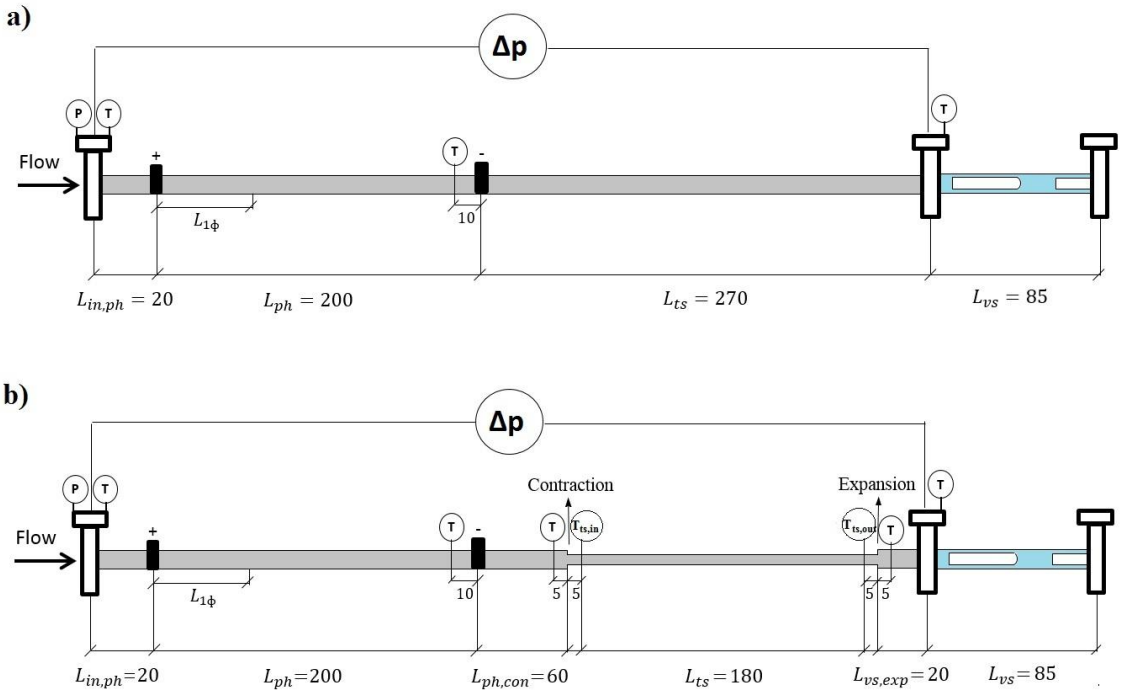

Figure 3. Schematic of the pre-heater and the test section for: a) circular channels and b) non-circular channels. (all dimension in mm.)

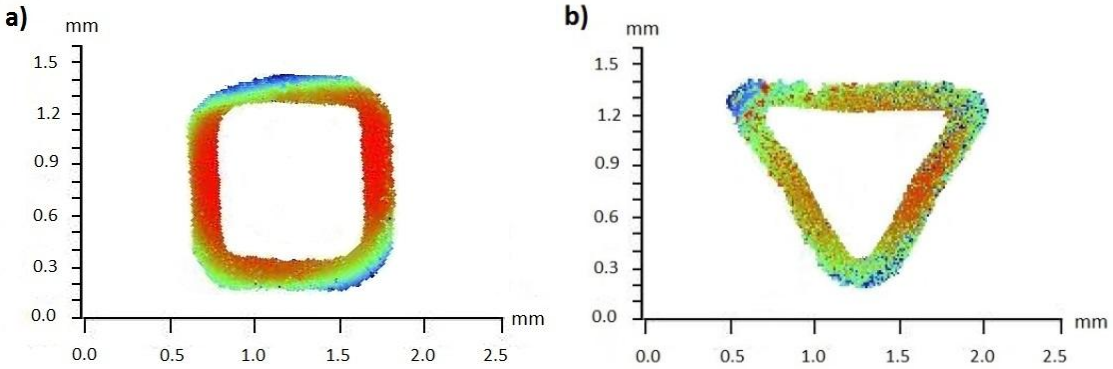

Figure 4. Cross-sectional geometries, a) Square channel, b) Triangular channel.

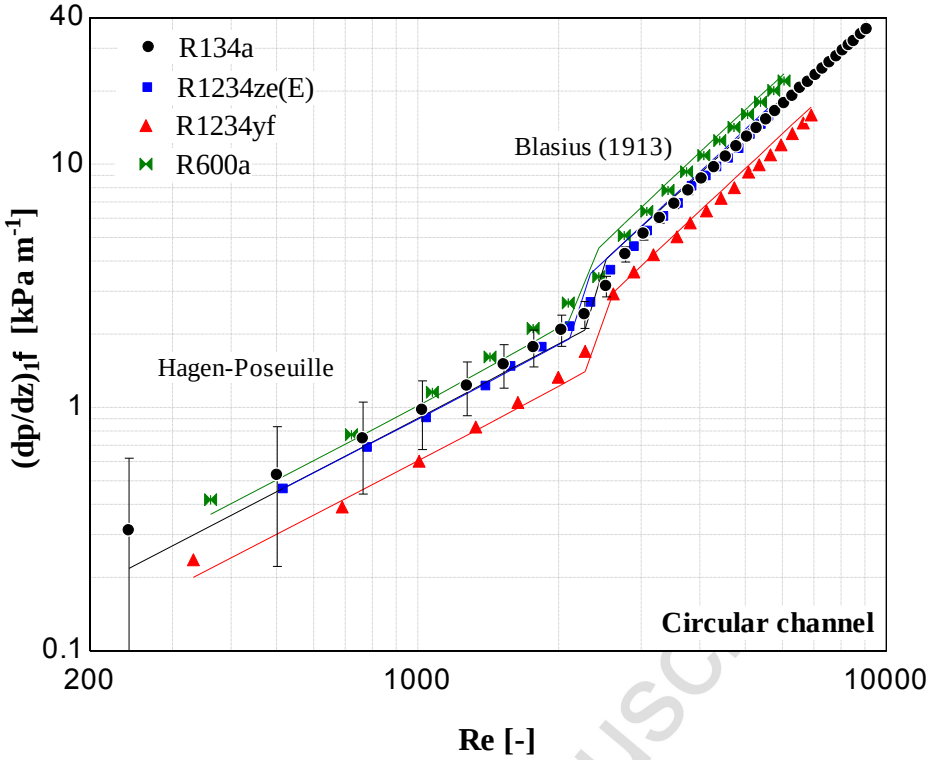

Figure 5. Comparison between experimental and estimated results for single-phase pressure drop for circular channels.

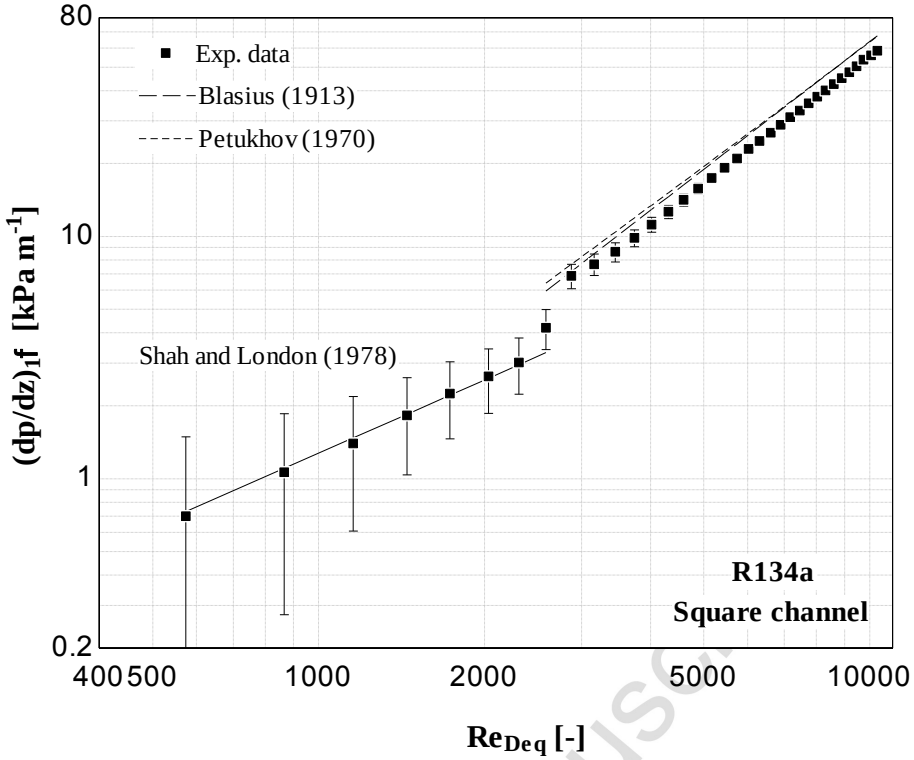

Figure 6. Comparison between predictions and experimental single-phase pressure drop for square channel.

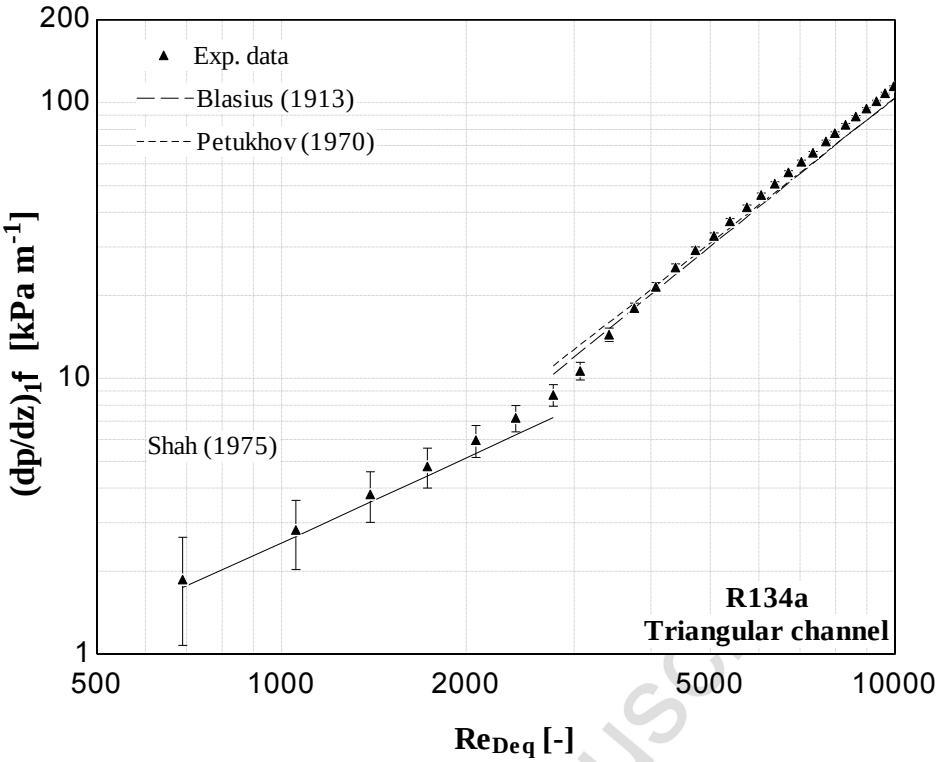

Figure 7. Comparison between predictions and experimental single-phase pressure drop for the triangular channel.

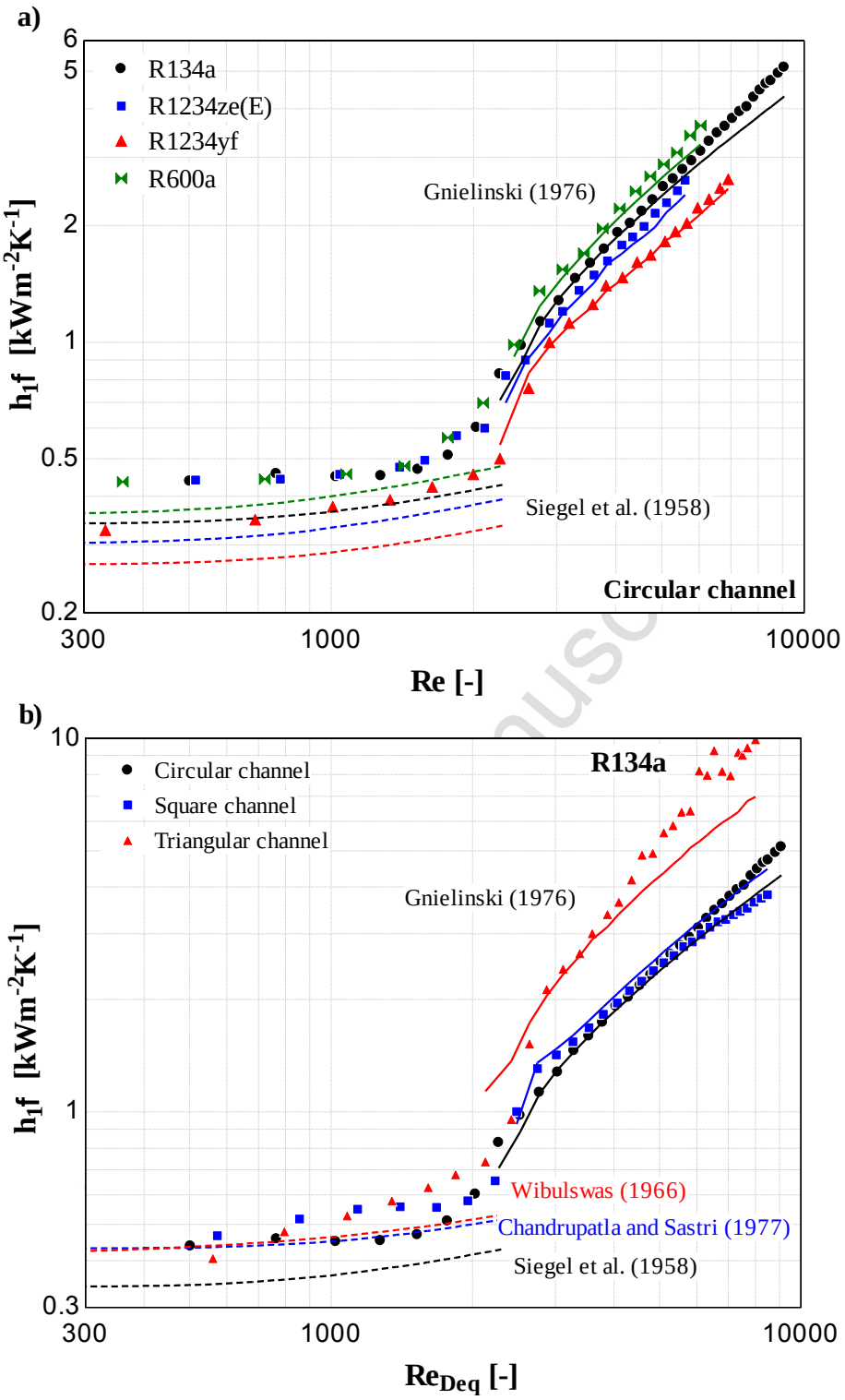

Figure 8. Comparison between predictions and experimental results for the heat transfer coefficient under single-phase flow conditions: a) refrigerant effect; b) channel geometry effect.

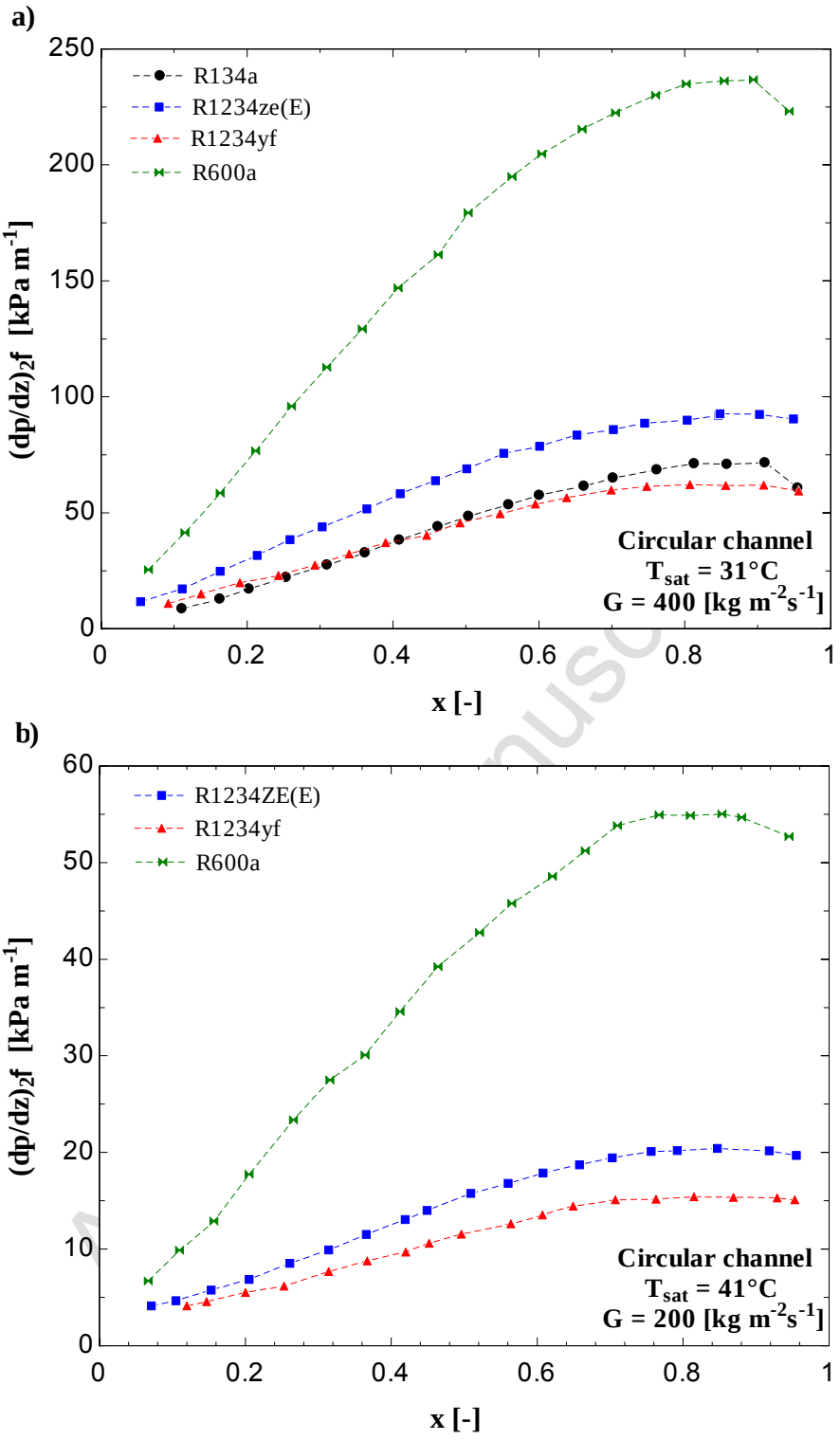

Figure 9. Effect of working fluid on the frictional pressure drop gradient.

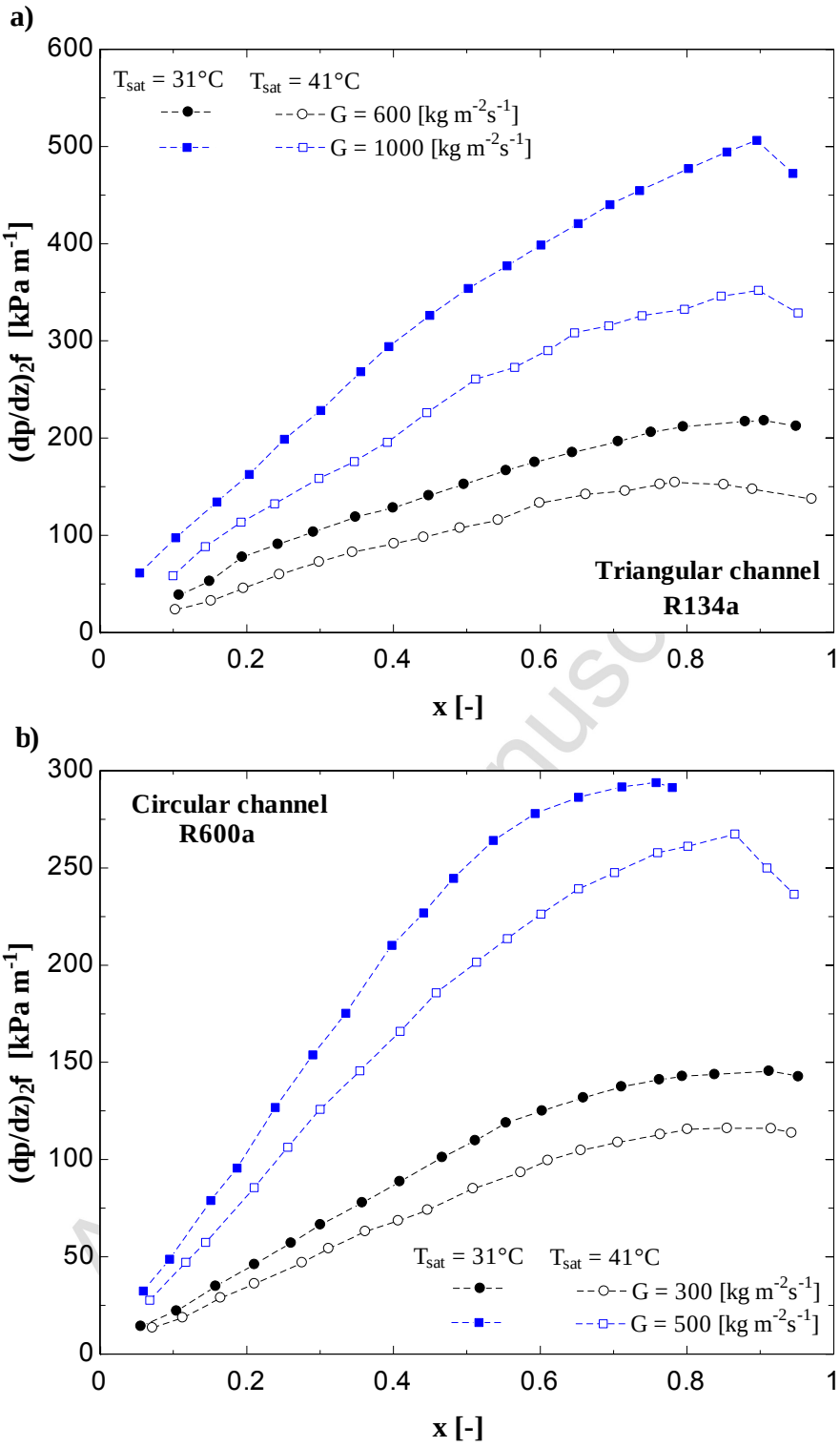

Figure 10. Effect of saturation temperature on the two-phase frictional pressure drop gradient.

a)

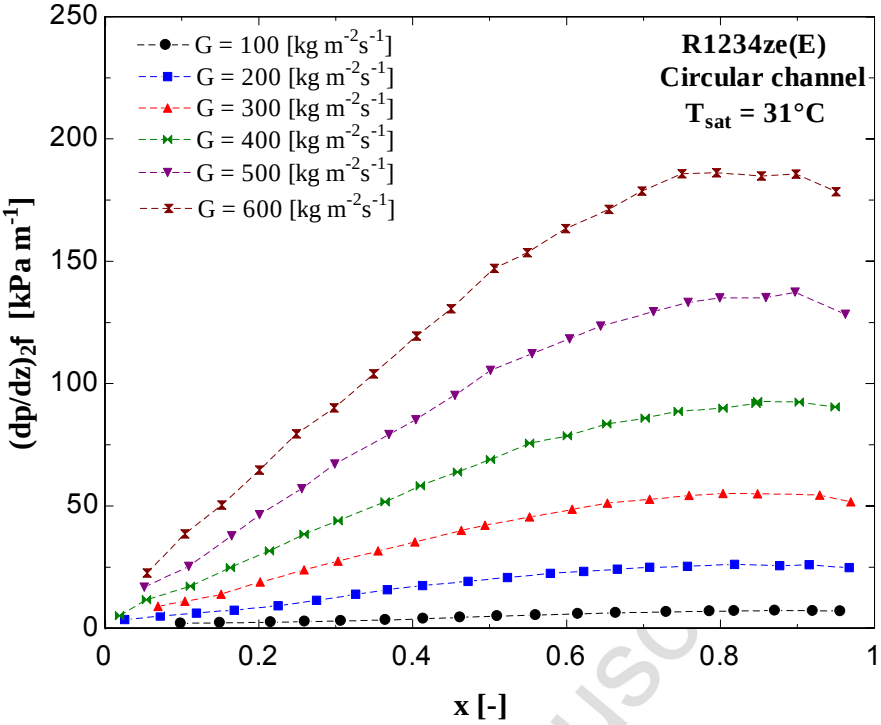

b)

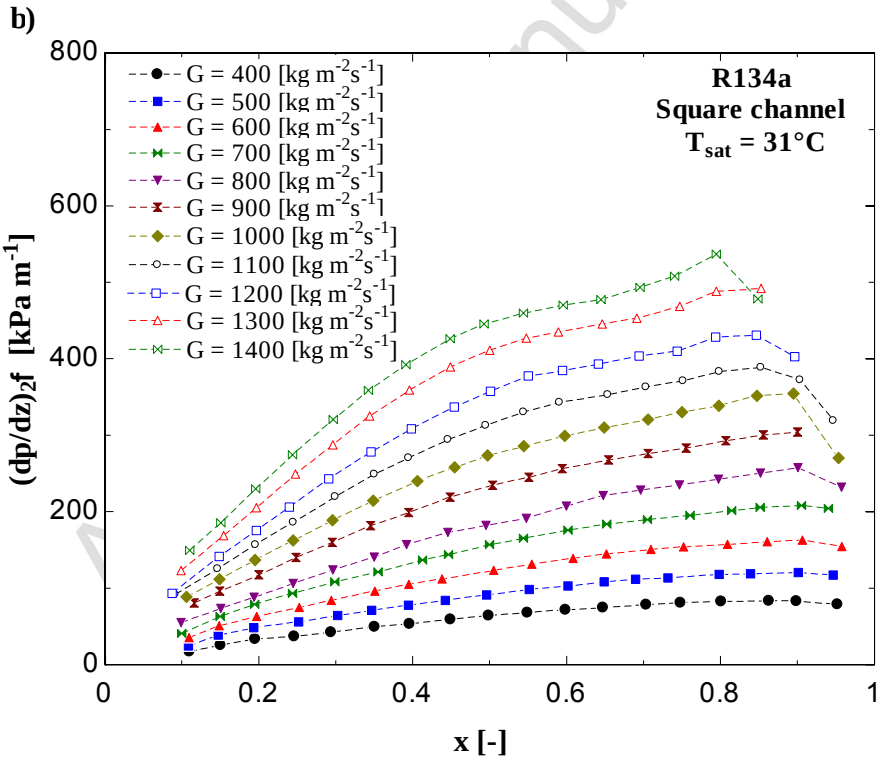

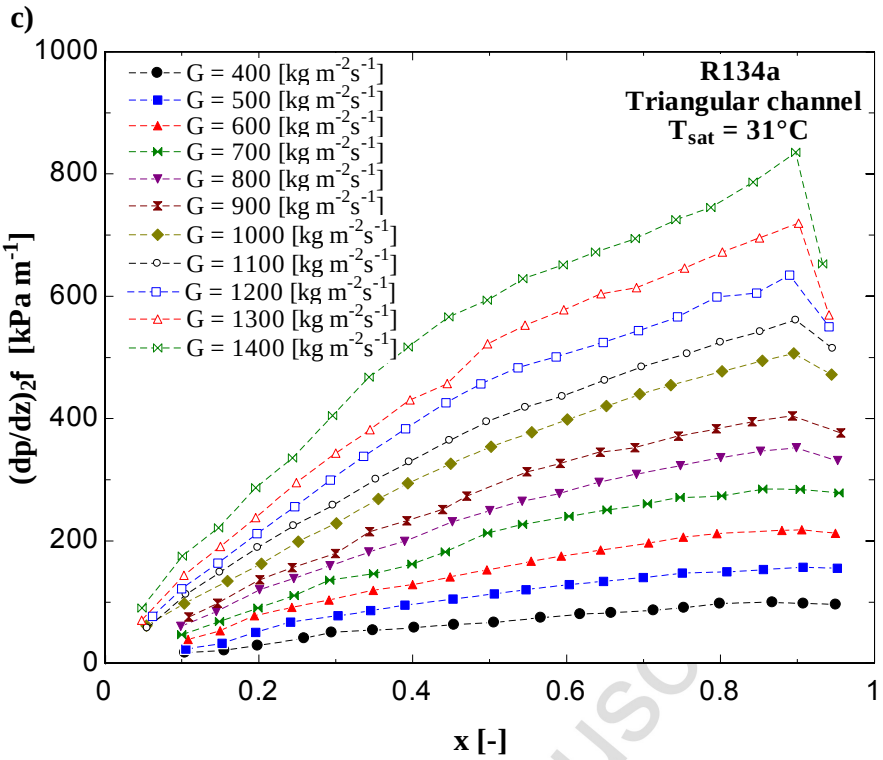

Figure 11. Effect of mass velocity and vapor quality on the two-phase frictional pressure drop gradient.

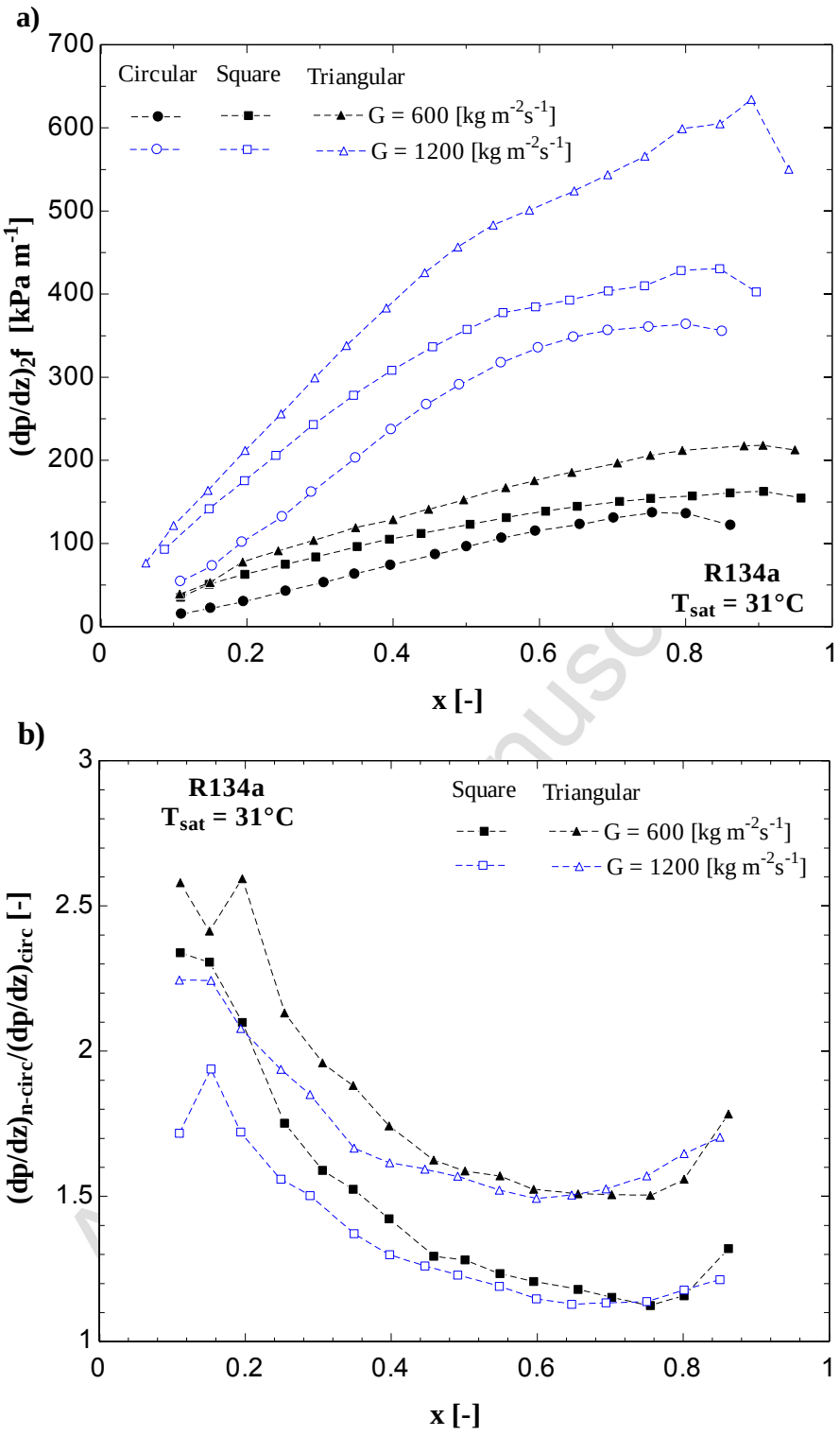

Figure 12. Effect of cross-sectional geometry on the two-phase frictional pressure drop gradient.

a)

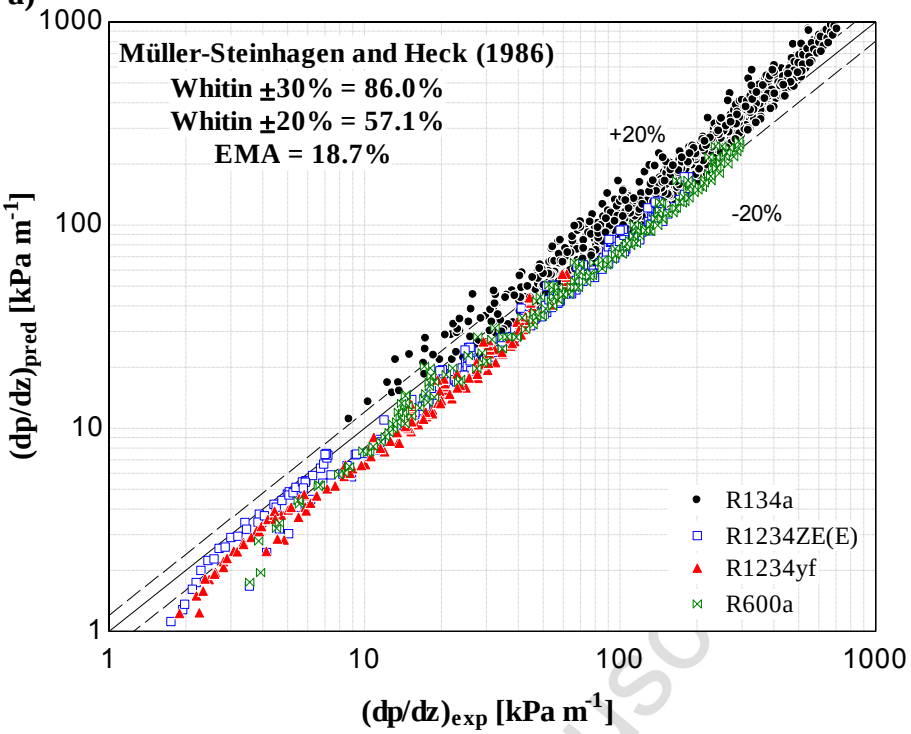

b)

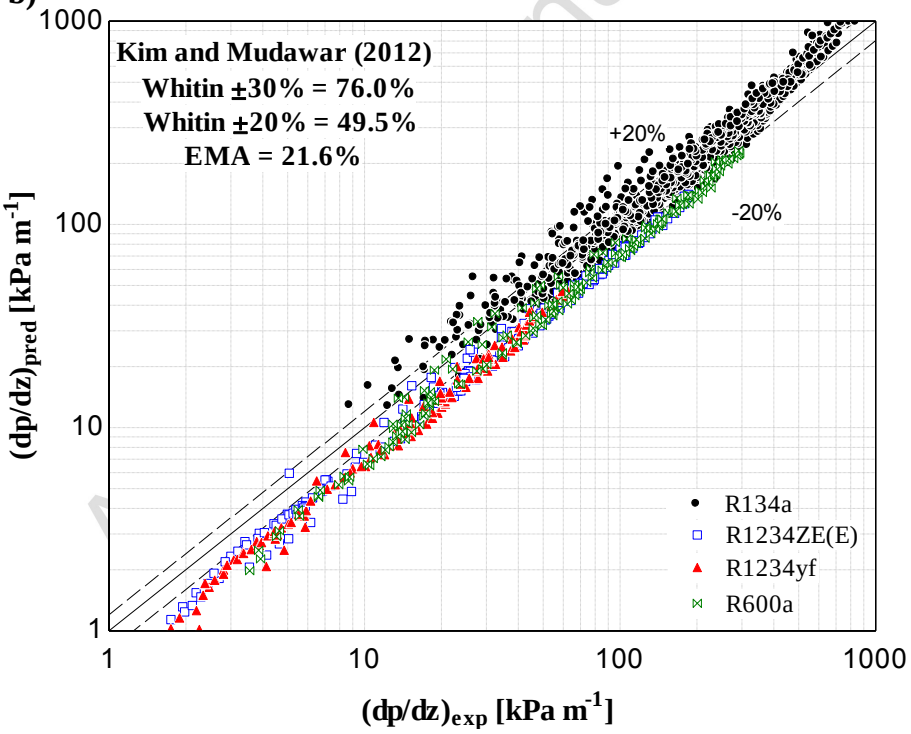

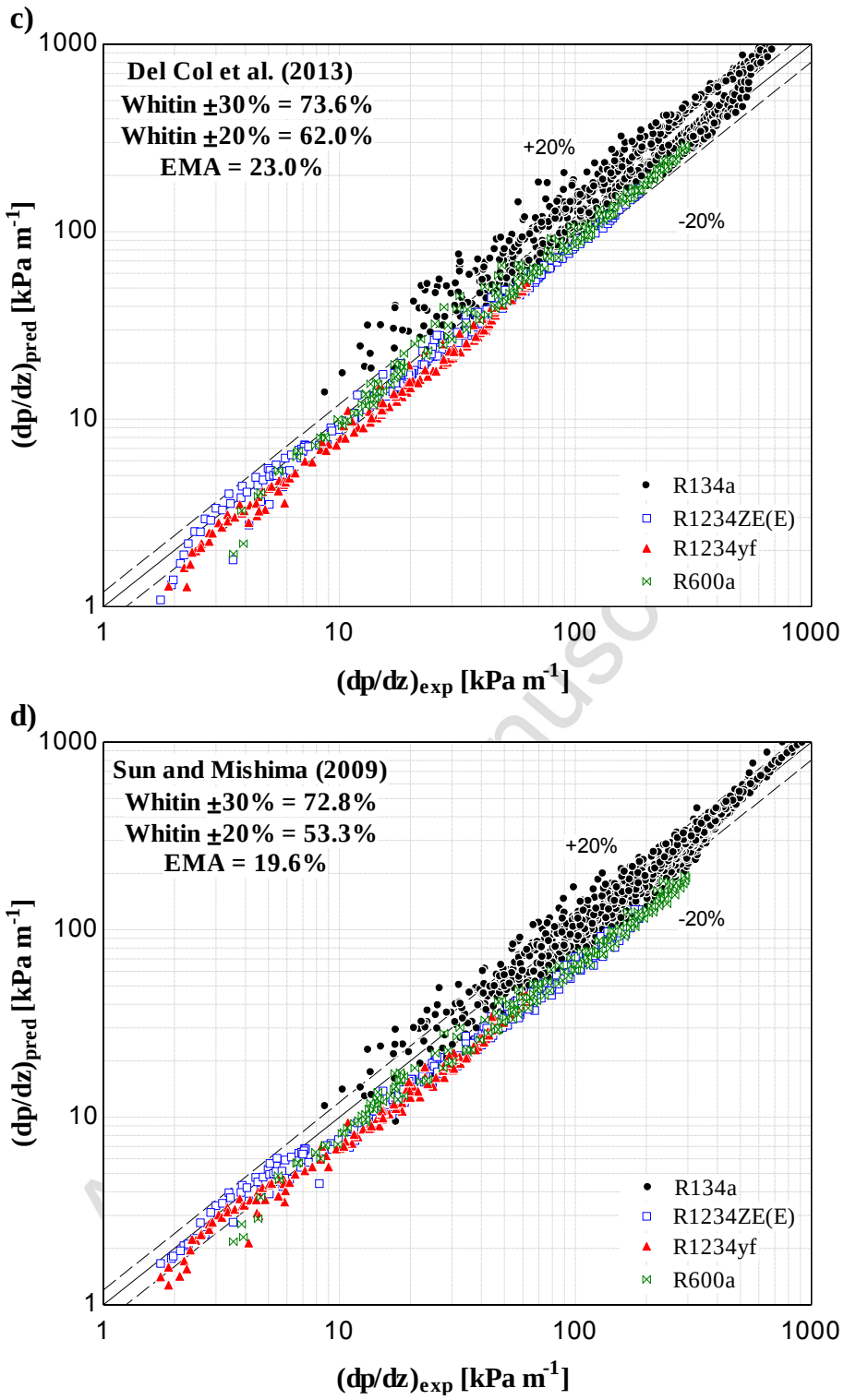

Figure 13. Comparison of the experimental database with prediction methods of: a) Müller-Steinhagen and Heck (1986), b) Kim and Mudawar (2012), c) Del Col et al. (2013), d) Sun and Mishima (2009).

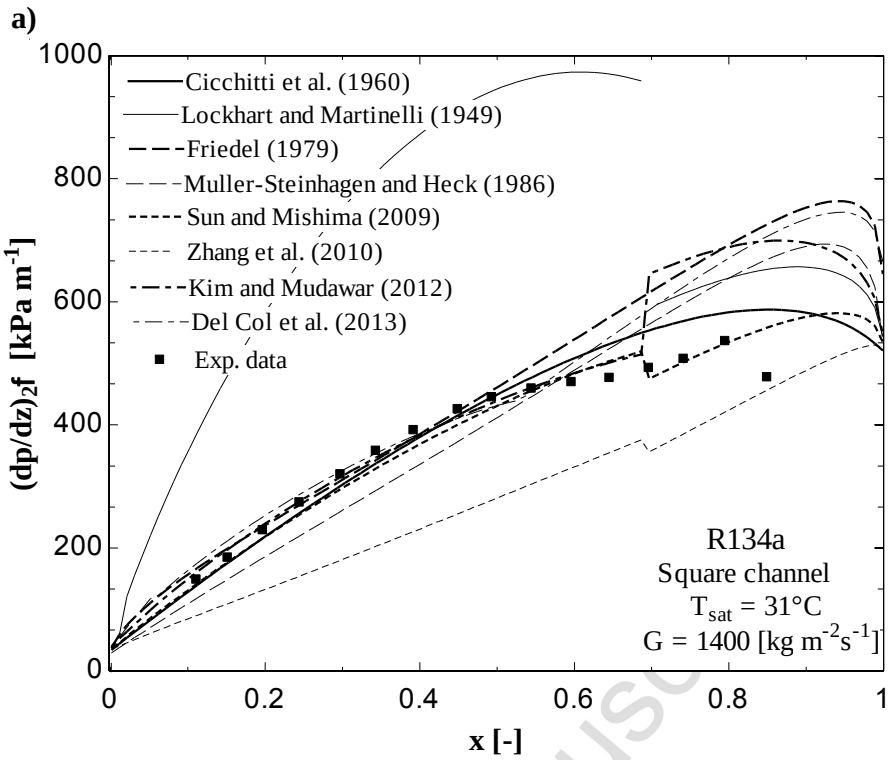

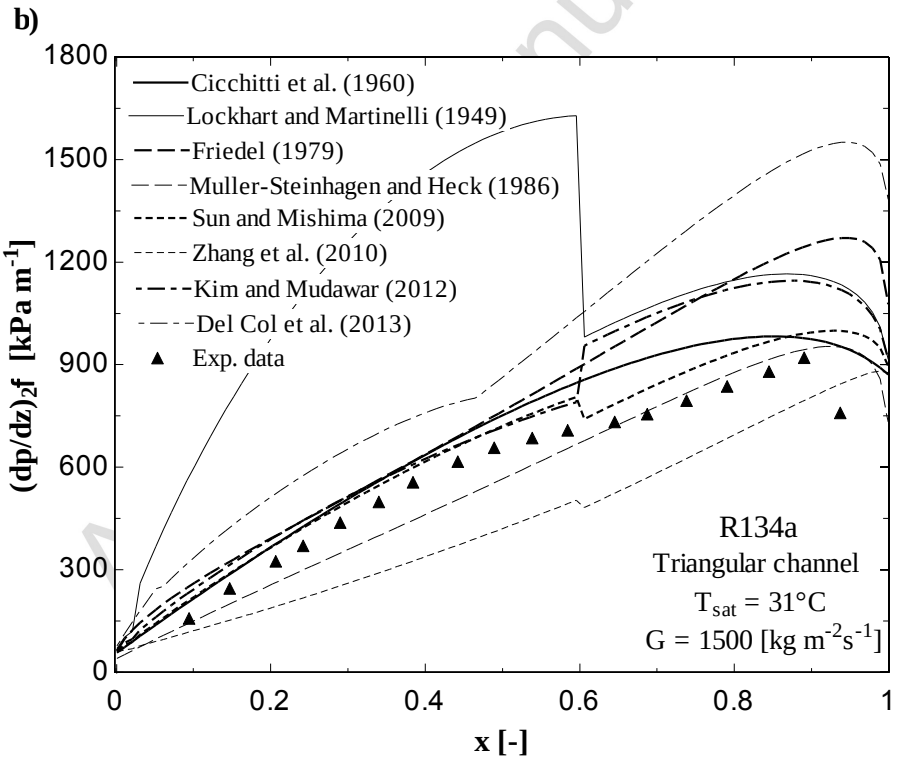

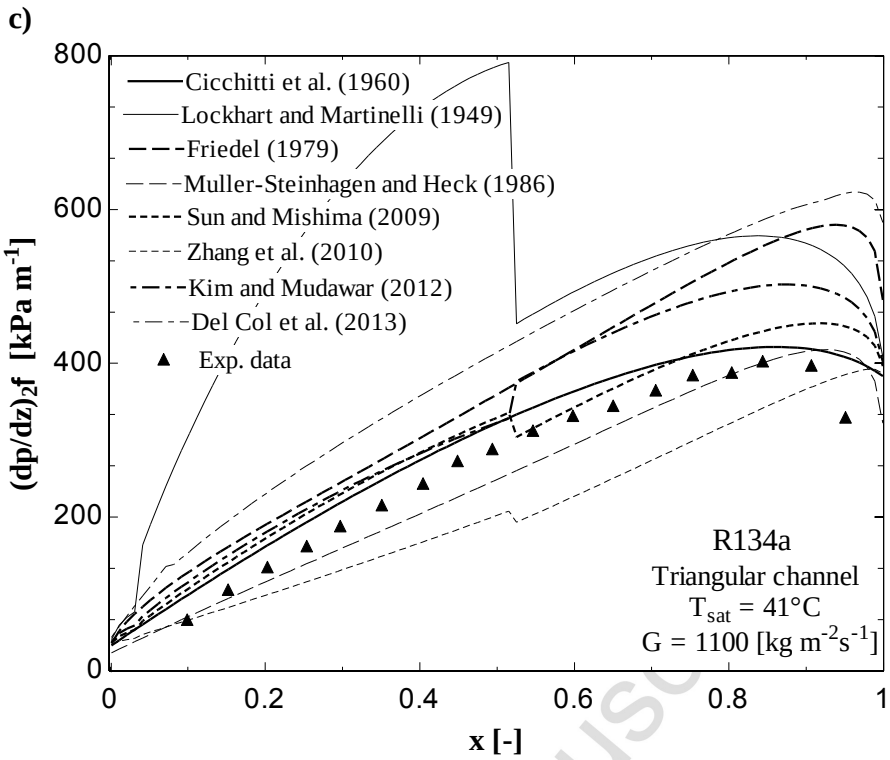

Figure 14. Comparison of frictional pressure drop trends according to predictive methods and the experimental data for non-circular channels.

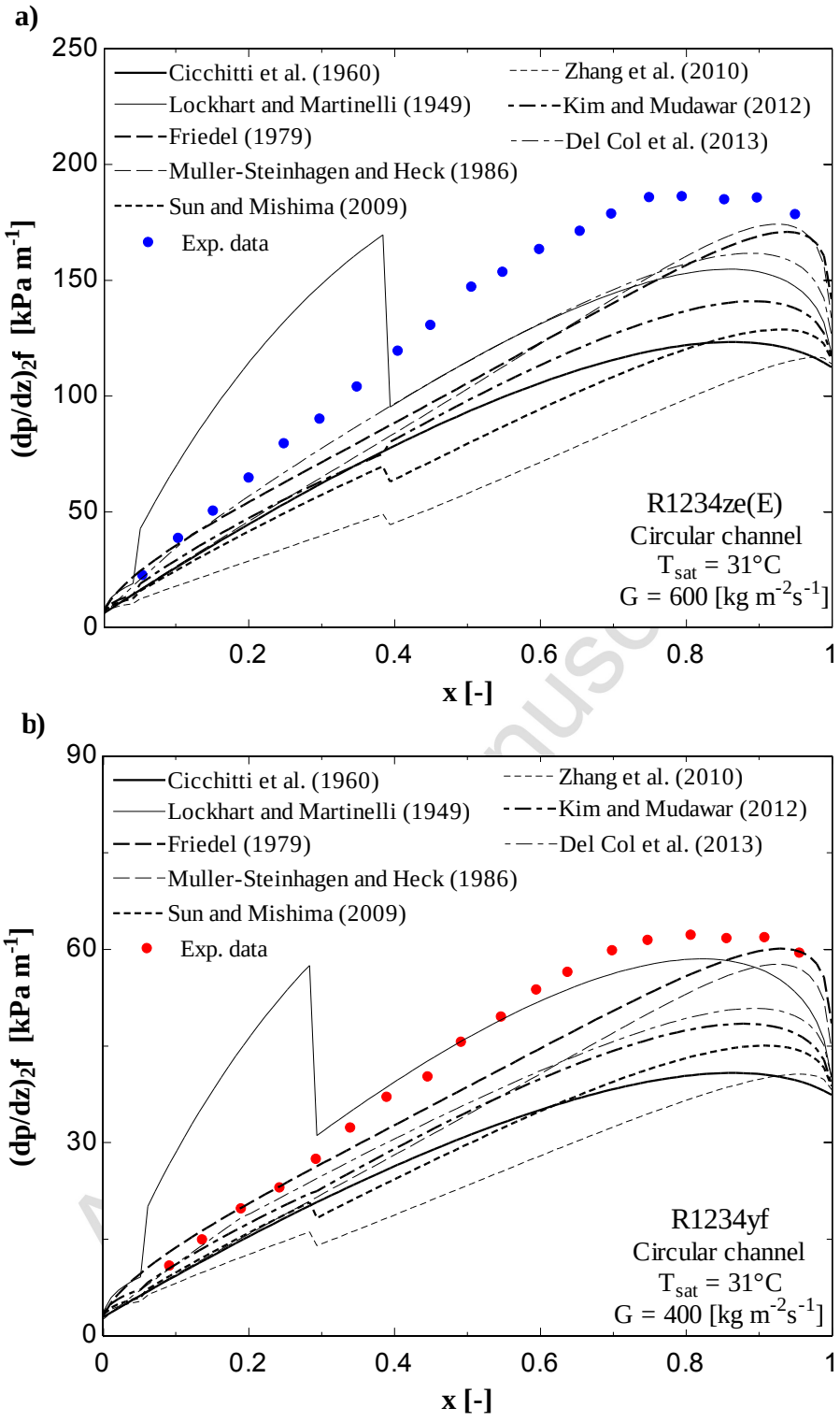

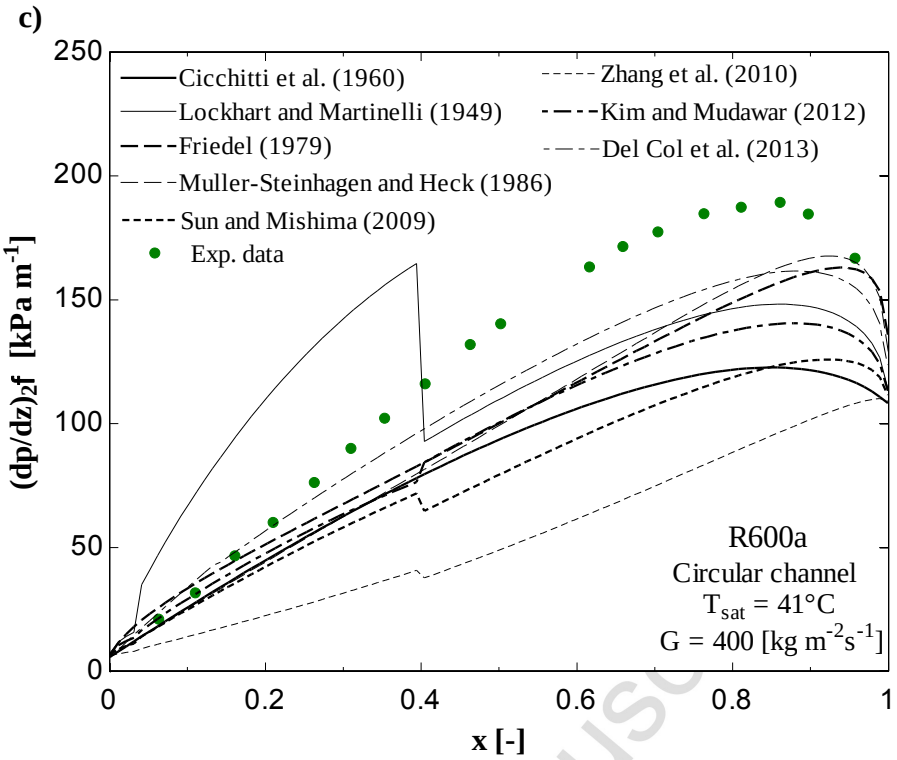

Figure 15. Comparison of frictional pressure drop trends according to predictive methods and the experimental data for circular channels.

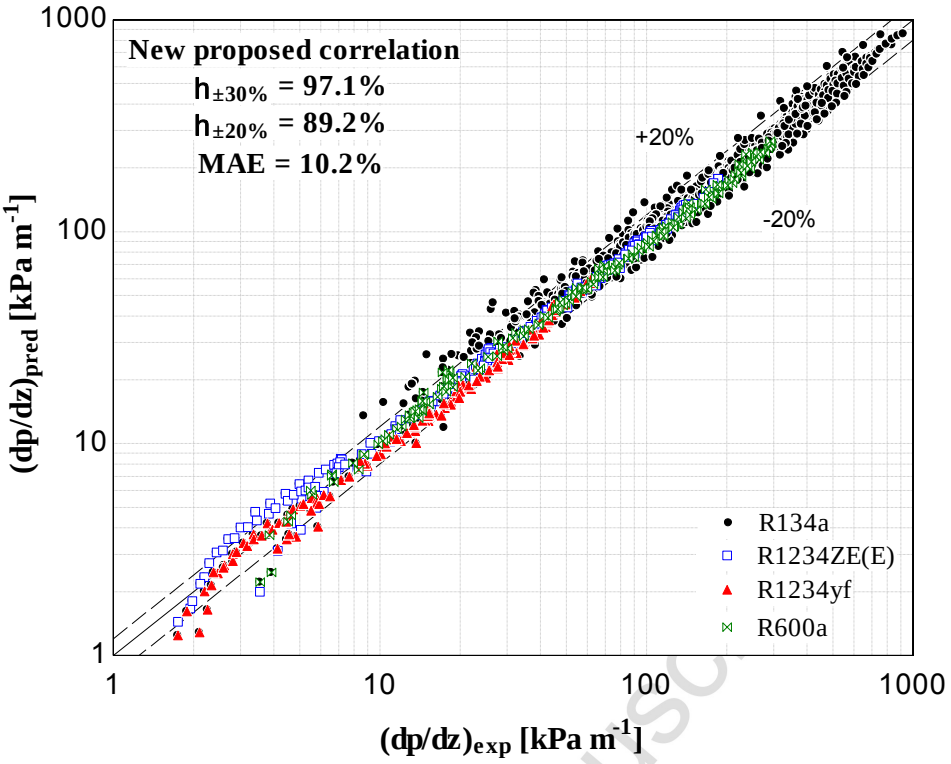

Figure 16. Comparison of the experimental database obtained in the present study and the new predictive method.

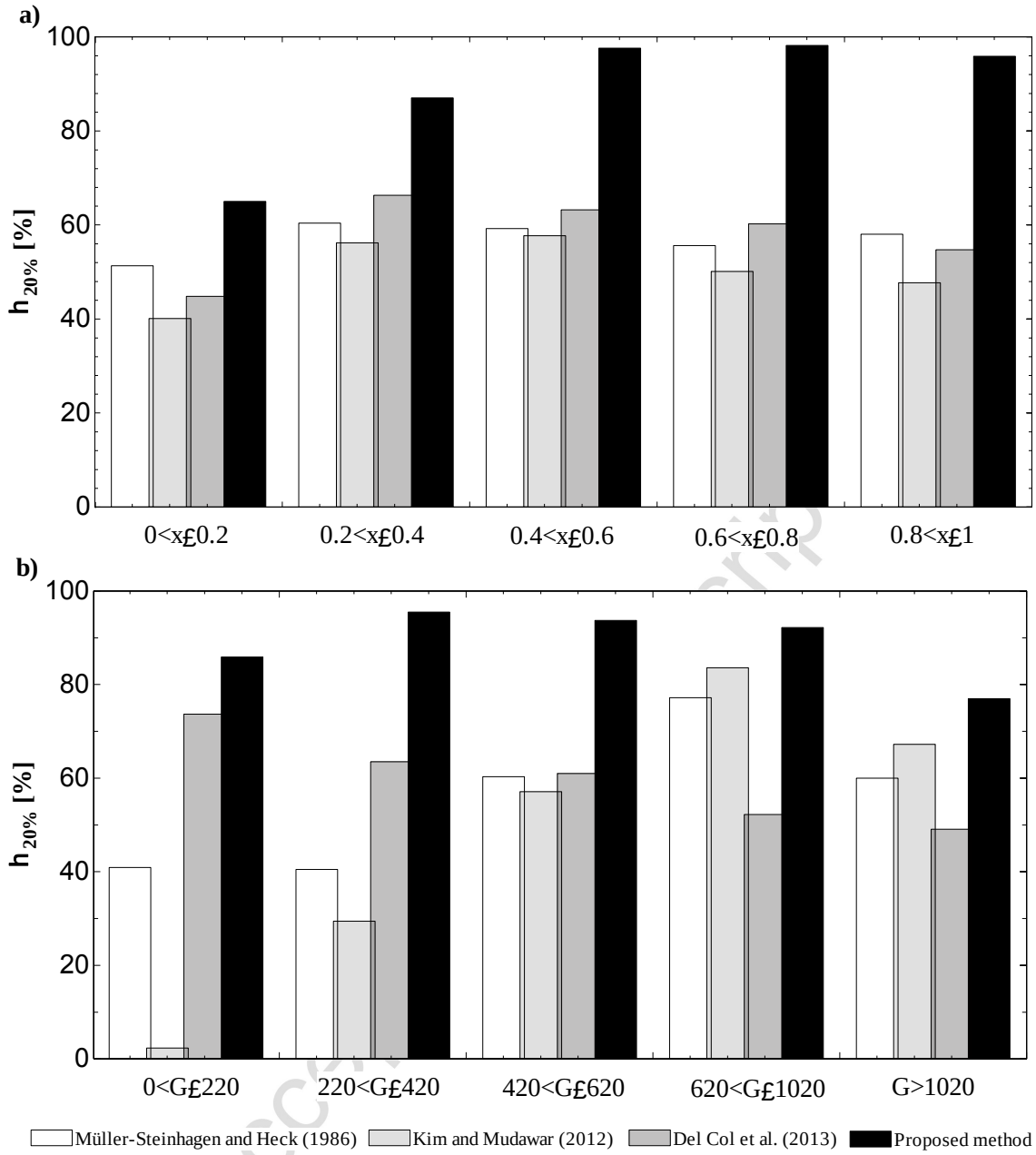

Figure 17. Parcel of data predicted within the ±20% of error band according vapor quality and mass velocity ranges.

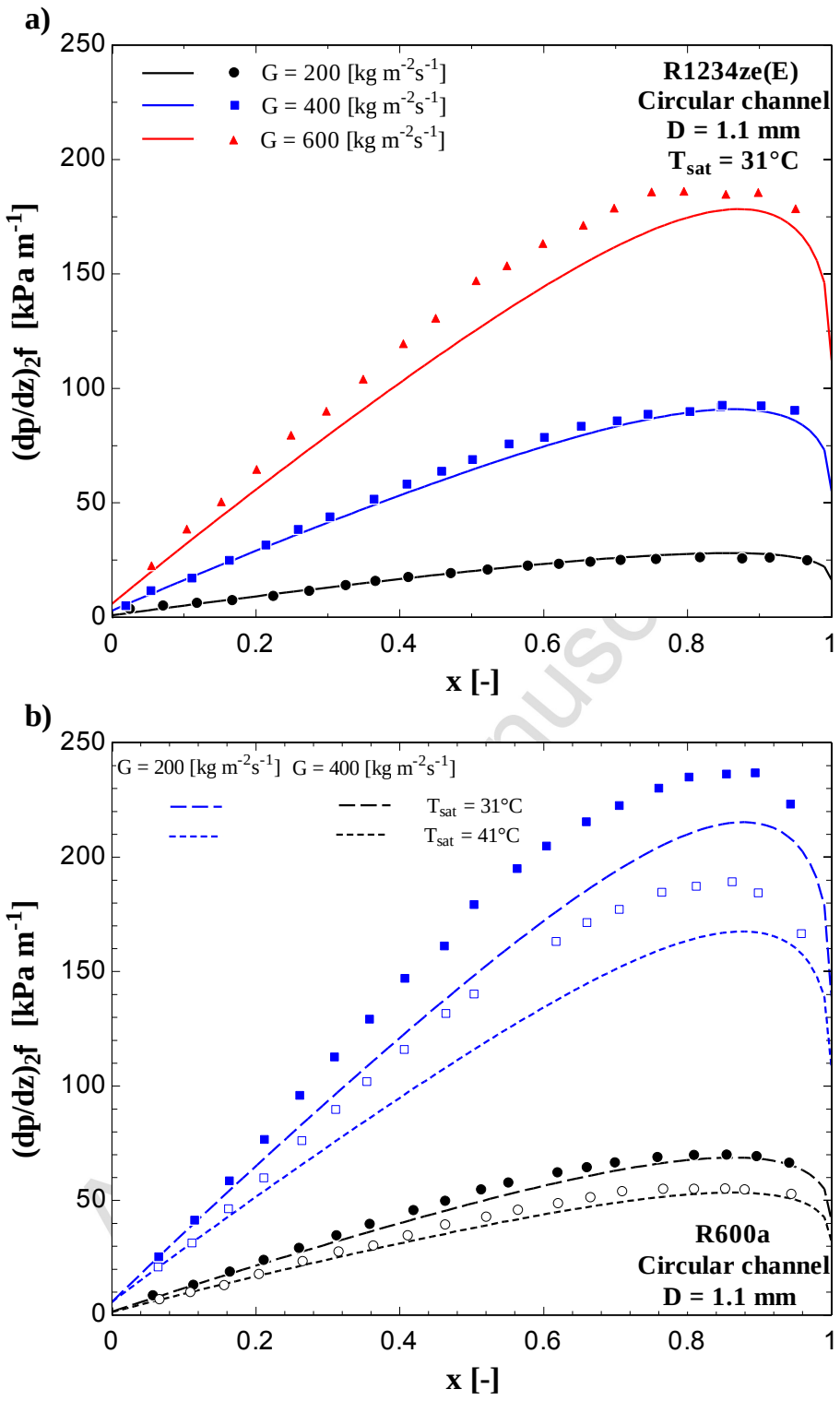

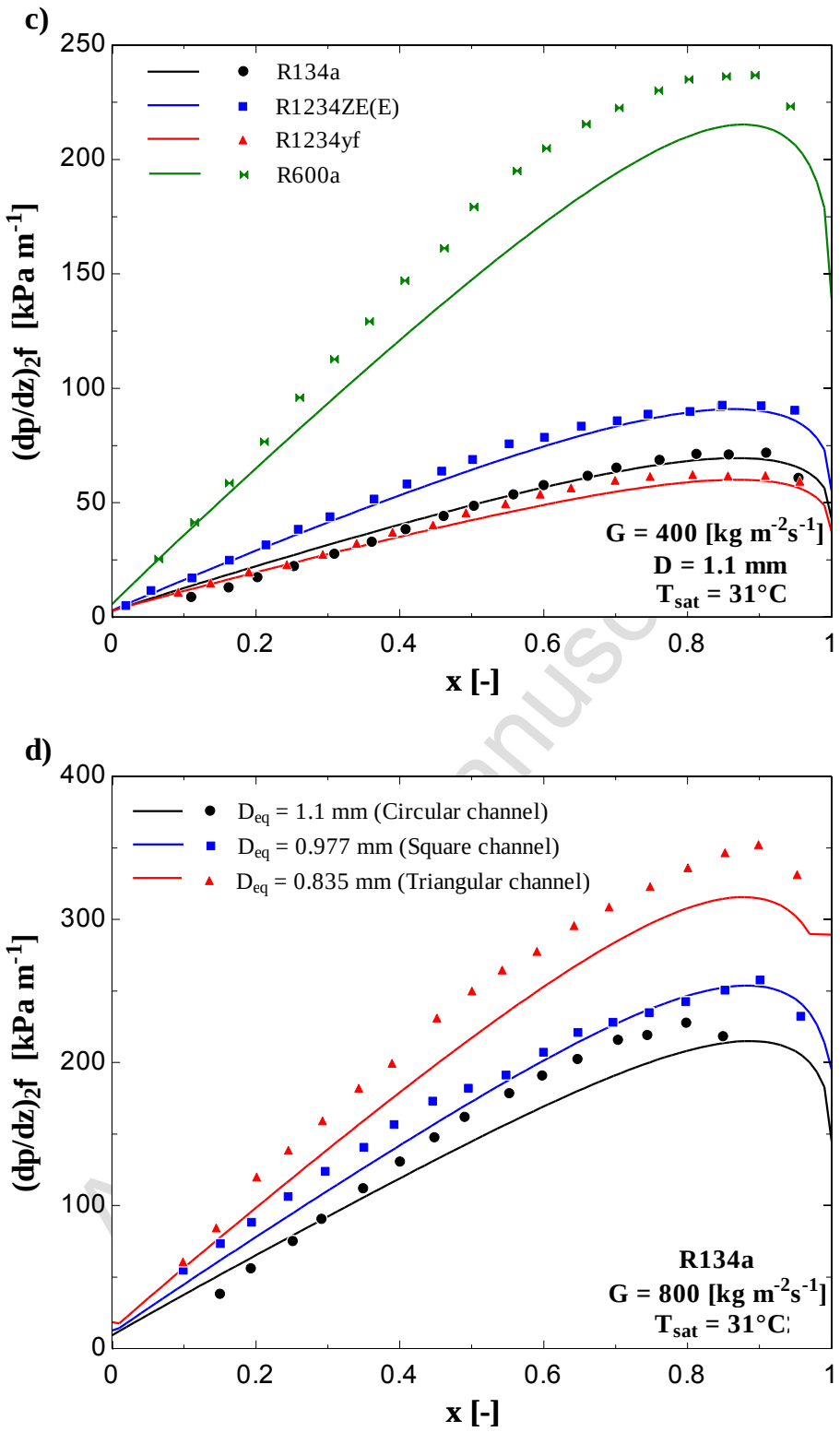

Figure 18. Comparison between experimental data and estimated trends according to the new predictive method.

Table 1. Experimental pressure drop studies for low GWP fluids in horizontal micro-scale channels.*

Author (s)	Conditions and Geometry	Fluid	D_H [mm]	G [kg m^{-2} s^{-1}] x [-]
Pamitran et al. (2010)	Diabatic/C Single channel	Propane, CO_2, NH_3	0,5, 1.5, 3	50 – 600 0 - 1
Ducoulombier et al. (2011)	Adiabatic/C Single channel	CO_2	0.529	200 – 1400 0 - 1
Wu et al. (2011)	Diabatic/C Single channel	CO_2	1.42	300 – 600 0 - 1
Del Col et al. (2013)	Adiabatic/S Single channel	R1234yf	1.23	200 – 800 0 - 1
Del Col et al. (2014)	Adiabatic/C Single channel	Propane	0.96	200 – 800 0 - 1
Del Col et al. (2015)	Adiabatic/C Single channel	R1234ze(E)	1.16	200 – 800 0 - 1
Huang et al. (2016)	Diabatic/S Multichannels	R1233zd(E)	0.1	500 – 2750 -

*** C → Circular, S → Square, T → Triangular.**

Table 2. Geometrical characteristics of the tes sections.*

Cross-sectional geometry	D_H [mm]	D_{eq} [mm]	ς [-]	*Ra* [μm]	*Rt* [μm]
Circular	1.1	1.1	-	0.289	4.45
Square	0.868	0.977	1.06	0.840	6.81
Triangular	0.634	0.835	-	1.780	8.31

*** Mean (average) value based on three measurements**

Table 3. Experimental conditions evaluated in the present study.

Working fluid	Cross-sectional geometry	D_H [mm]	D_{eq} [mm]	T_{sat} [°C]	G [kg m^{-2} s^{-1}]	x [-]	$(dp/dz)_{exp}$ [kPa m^{-1}]
R134a	Circular	1.1	1.1	31, 41	400 - 1600	0.1 – 0.95	8.7 - 411.4
	Square	0.868	0.977	31, 41	400 - 1600	0.1 – 0.95	13.7 – 610.3
	Triangular	0.634	0.835	31, 41	400 - 1400	0.1 – 0.95	12.3 – 920.5
R1234ze(E)	Circular	1.1	1.1	31, 41	100 - 600	0.05 – 0.95	1.75 – 186.1
R1234yf	Circular	1.1	1.1	31, 41	100 - 400	0.05 – 0.95	1.74 – 62.2
R600a	Circular	1.1	1.1	31, 41	100 - 500	0.05 – 0.95	3.55 – 293.8

Table 4. Uncertainties of measured and calculated parameters.

Measured parameter	Uncertainty	Calculated parameter	Uncertainty
D	20 µm	D_{eq} ■▲	< 20 µm
L_{ph}, L_{ts}	1 mm	x	< 5%
p_{in}	4.5 kPa	G	< 2%
Δp	150 Pa	$(dp/dz)_{2\phi}$ ■▲*	< 15%
P_{ph}	0.8 %	$(dp/dz)_{2\phi}$ ●	< 10%
T	0.15 °C		
$\dot{m}$	0.1 %		

***80% of the experimental data.**

Table 5. Mean absolute error (MAE) and the parcel of predictions (η) within an error band of ±20% of the measurements.*

Exp. database	Cross-sectional geometry	Data points		Predictive methods										
				Hom-Cicchitti et al. (1960)	**Hom - Dukler et al.** (1964)	**Lockart and Martinelli** (1949)	**Friedel** (1979)	**Müller-Steinhagen and Heck** (1986)	**Cioncolini et al.** (2009)	**Sun & Mishima** (2009)	**Zhang et al.** (2010)	**Li and Wu** (2011)	**Kim and Mudawar** (2012)	**Del Col et al.** (2013)
R134a	Circular	253	MAE	**18.7%**	36.2%	100.2%	**17.7%**	**13.6%**	41.4%	20.7%	33.0%	45.2%	**18.5%**	**18.1%**
			η	54.5%	14.6%	35.6%	77.9%	**81.0%**	18.2%	49.4%	17.0%	17.4%	68.8%	79.8%
R134a	Square	295	MAE	**10.7%**	34.9%	69.7%	**13.2%**	**16.7%**	39.2%	**12.1%**	37.3%	40.4%	**15.8%**	**11.0%**
			η	**89.2%**	7.1%	35.9%	75.6%	60.3%	37.6%	**82.4%**	8.5%	25.1%	71.2%	**87.8%**
R134a	Triangular	365	MAE	**10.2%**	23.7%	89.3%	25.6%	**15.1%**	33.3%	**11.2%**	32.4%	45.4%	**18.0%**	56.0%
			η	**90.1%**	29.9%	4.4%	41.9%	67.9%	43.8%	**87.1%**	18.1%	16.7%	54.8%	0.0%
R1234ze(E)	Circular	229	MAE	31.9%	49.2%	30.2%	25.5%	**19.0%**	45.2%	27.8%	43.3%	29.7%	28.7%	**14.2%**
			η	8.7%	0.4%	65.5%	59.4%	44.1%	19.2%	18.8%	4.8%	59.0%	7.0%	**80.8%**
R1234yf	Circular	140	MAE	38.5%	52.7%	29.0%	**19.9%**	26.1%	39.0%	28.5%	39.4%	25.7%	30.9%	22.6%
			η	0.7%	0.0%	57.9%	52.1%	25.0%	33.6%	21.4%	5.0%	54.3%	6.4%	36.4%
R600a	Circular	186	MAE	28.1%	50.3%	31.6%	21.3%	20.4%	49.1%	29.5%	56.4%	20.1%	26.6%	**11.3%**
			η	16.7%	0.0%	41.92%	43.3%	41.4%	10.8%	21.0%	0.0%	68.8%	14.5%	**94.1%**
Overall		1468	MAE	20.1%	38.2%	65.0%	20.7%	**17.5%**	40.3%	**19.6%**	38.9%	36.8%	21.6%	23.1%
			η	53.3%	11.4%	35.5%	58.7%	57.5%	29.2%	54.4%	10.4%	35.3%	49.5%	63.8%

***Bold numbers indicate a Mean Average Error (MAE) below 20% and more than 80% of the data predicted within the ±20% of the measurement.**

Table 6. Schematic of the new predictive for frictional pressure drop inside small diameter channels.

$$\left(\frac{dp}{dz}\right)_{2\phi} = F\cdot\left(1-x\right)^{1/\lambda} + \left(\frac{dp}{dz}\right)_{G0}\cdot x^{\lambda}$$

$$F = \left(\frac{dp}{dz}\right)_{L0} + \omega\cdot\left(\left(\frac{dp}{dz}\right)_{G0} - \left(\frac{dp}{dz}\right)_{L0}\right)\cdot x \qquad D_{eq} = \sqrt{\frac{4A}{\pi}} \qquad \left(\frac{dp}{dz}\right)_{k0} = 2\,f_{k0}\,\frac{G^2}{D_{eq}\cdot\rho_k}$$

The coefficients of Eq. (21) given by:

$$\omega = a\cdot e^{b\cdot \mathrm{Re}_{G0}/1000};\ \lambda = 2.31$$

$$a = 3.01;\ b = -0.00464$$

For laminar flow:

Circular channel: $f_{k0} = \dfrac{16}{\mathrm{Re}_{k0}}$

Rectangular channel: $f_{k0} = \dfrac{24\left(1-1,3553\varsigma+1,9467\varsigma^2-1,7012\varsigma^3+0,9564\varsigma^4-0,2537\varsigma^5\right)}{\mathrm{Re}_{k0}}\cdot\dfrac{D_{eq}}{D_H}$

Triangular channel: $f_{k0} = \dfrac{13.333}{\mathrm{Re}_{k0}}\cdot\dfrac{D_{eq}}{D_H}$ (sharp corners) $f_{k0} = \dfrac{15.993}{\mathrm{Re}_{k0}}\cdot\dfrac{D_{eq}}{D_H}$ (3 rounded corners)

For turbulent flow regardless of the cross-sectional geometry:

$$f_{k0} = 0.0791\,\mathrm{Re}_{k0}^{-0.25}$$

The Reynolds number is calculated using the equivalent diameter as the characteristic dimension:

$$\mathrm{Re}_{k0} = \frac{GD_{eq}}{\mu_k}$$

where subscript *k* denotes *L* or G for liquid and vapor phases, respectively.

Table 7. Stadistical parameters from the comparison between the present experimental data and the predictions of the new method.*

Exp. database	Cross-sectional geometry	Data points	MAE	MRE	$\eta_{30\%}$	$\eta_{20\%}$
R134a	Circular	253	**11.4%**	**4.0%**	**90.9%**	**85.0%**
R134a	Square	295	**11.9%**	**-7.0%**	**99.0%**	**80.0%**
R134a	Triangular	365	**9.7%**	**-5.7%**	**98.9%**	**93.7%**
R1234ze(E)	Circular	229	**8.0%**	**-1.0%**	**97.4%**	**91.3%**
R1234yf	Circular	140	**10.7%**	**-9.7%**	**97.9%**	**92.9%**
R600a	Circular	186	**9.3%**	**-6.5%**	**98.9%**	**97.8%**
Overall		1468	**10.2%**	**-4.0%**	**97.2%**	**89.2%**

***Bold numbers indicate a MAE below 20%, MRE below ±10%, $\eta_{30\%}$ more than 90% and $\eta_{20\%}$ more than 80%.**

Table 8. Statistical parameters from the comparison between independent databases and the predictions by the new method.*

Author (s)	Fluid/Diameter	Geometry	# Data	MAE	$\eta_{30\%}$	$\eta_{20\%}$
Del Col et al. (2013)	R1234yf D_{eq} = 1.388 mm	Square	42	**16.1%**	88.7%	64.0%
Del Col et al. (2015)	R1234ze(E) D = 0.96 mm	Circular	52	**15.1%**	**90.4%**	75.0%
Ducoulombier et al. (2011)	CO_2 D = 0.529 mm	Circular	281	**12.7%**	89.3%	78.6%
Del Col et al. (2014)	Propano D = 0.96 mm	Circular	48	**7.2%**	**100%**	**95.8%**
Overall			423	**12.7%**	**90.5%**	78.5%

***Bold numbers indicate a MAE below 20%, $\eta_{30\%}$ more than 90% and $\eta_{20\%}$ more than 80%.**